Costs of dust collection by *Trichodesmium*: effect on buoyancy and toxic metal release

Siyuan Wang[1], Futing Zhang[1], Coco Koedooder[2], Odeta Qafoku[3], Subhajit Basu[4], Stephan Krisch[5], Anna-Neva Visser[1], Meri Eichner[6], Nivi Kessler[7], Rene Boiteau[8], Martha Gledhill[9], and Yeala Shaked[10]

[1]The Hebrew University of Jerusalem & The Interuniversity Institute for Marine Sciences in Eilat
[2]The Hebrew University of Jerusalem, The Interuniversity Institute for Marine Sciences in Eilat & Israel Limnology and Oceanography Research
[3]Pacific Northwest National Laboratory
[4]The Hebrew University of Jerusalem, The Interuniversity Institute for Marine Sciences in Eilat & UPES, Dehradun
[5]Bundesanstalt für Gewässerkunde
[6]Institute of Microbiology of the Czech Academy of Sciences
[7]The Hebrew University of Jerusalem, The Interuniversity Institute for Marine Sciences in Eilat & The water authority, Israel
[8]Massachusetts Institute of Technology
[9]GEOMAR Helmholtz Center for Ocean Research
[10]Hebrew University & Interuniversity Inst for Marine Sciences

December 10, 2023

Abstract

The marine cyanobacterium *Trichodesmium* has a remarkable ability to interact with and utilize air-borne dust as a nutrient source. However, dust may adversely affect *Trichodesmium* through buoyancy loss and exposure to toxic metals. Our study explored the effect of desert dust on buoyancy and mortality of natural Red Sea puff-shaped *Trichodesmium thiebautii*. Sinking velocities and ability of individual colonies to stay afloat with increasing dust loads were studied in sedimentation chambers. Low dust loads of up to ~400 ng per colony did not impact initial sinking velocity and colonies remained afloat in the chamber. Above this threshold, sinking velocity increased linearly with the colony dust load at a slope matching prediction based on Stoke's law. The potential toxicity of dust was assessed with regards to metal dissolution kinetics, differentiating between rapidly released metals that may impact surface blooms and gradually released metals that may impact dust-centering colonies. Incubations with increasing dust concentrations revealed colony demise, but the observed lethal dose far exceeded dust concentrations measured in coastal and open ocean systems. Removal of toxic particles as a mechanism to reduce toxicity was explored using SEM-EDX imaging of colonies incubated with Cu-minerals, yet observations did not support this pathway. Combining our current and former experiments, we suggest that in natural settings the nutritional benefits gained by *Trichodesmium* via dust collection outweigh the risks of buoyancy loss and toxicity. Our data and concepts feed into the growing recognition of the significance of dust for *Trichodesmium*'s ecology and subsequently to ocean productivity.

Posted on 10 Dec 2023 — The copyright holder is the author/funder. All rights reserved. No reuse without permission. — https://doi.org/10.22541/essoar.170224456.62975053/v1 — This is a preprint and has not been peer-reviewed. Data may be preliminary.

Costs of dust collection by *Trichodesmium*: effect on buoyancy and toxic metal release

Siyuan Wang [1,2], Futing Zhang [1,2], Coco Koedooder [1,2,3], Odeta Qafoku [4], Subhajit Basu [1,2,5], Stephan Krisch [8], Anna-Neva Visser [1,2], Meri Eichner [6], Nivi Kessler [1,2,9], Rene M. Boiteau [7], Martha Gledhill [8] and Yeala Shaked [1,2]

[1] The Freddy and Nadine Herrmann Institute of Earth Sciences, Edmond J. Safra Campus, Givat Ram, Hebrew University of Jerusalem, Jerusalem, Israel

[2] The Interuniversity Institute for Marine Sciences in Eilat, Eilat, Israel

[3] Israel Limnology and Oceanography Research, Haifa, Israel

[4] Environmental Molecular Sciences Laboratory (EMSL), Pacific Northwest National Laboratory (PNNL), Richland, WA, 99454, USA

[5] University of Petroleum and Energy Studies (UPES-SoHST), Energy Acres, Dehradun 248007, India

[6] Center Algatech, Institute of Microbiology of the Czech Academy of Sciences, Novohradská 237, 37981 Třeboň, Czech Republic

[7] Department of Chemistry, University of Minnesota, Minneapolis, MN 55455

[8] GEOMAR, Helmholtz Center for Ocean Research, Kiel, Germany

[9] Present address: The water authority, 7 Bank of Israel st, Jerusalem 9195021, Israel

Corresponding author: Yeala Shaked

Email: yeala.shaked@mail.huji.ac.il

Abstract

The marine cyanobacterium *Trichodesmium* has a remarkable ability to interact with and utilize air-borne dust as a nutrient source. However, dust may adversely affect *Trichodesmium* through buoyancy loss and exposure to toxic metals. Our study explored the effect of desert dust on buoyancy and mortality of natural Red Sea puff-shaped *Trichodesmium thiebautii*. Sinking velocities and ability of individual colonies to stay afloat with increasing dust loads were studied in sedimentation chambers. Low dust loads of up to ~400 ng per colony did not impact initial sinking velocity and colonies remained afloat in the chamber. Above this threshold, sinking velocity increased linearly with the colony dust load at a slope matching prediction based on Stoke's law. The potential toxicity of dust was assessed with regards to metal dissolution kinetics, differentiating between rapidly released metals that may impact surface blooms and gradually released metals that may impact dust-centering colonies. Incubations with increasing dust concentrations revealed colony demise, but the observed lethal dose far exceeded dust concentrations measured in coastal and open ocean systems. Removal of toxic particles as a mechanism to reduce toxicity was explored using SEM-EDX imaging of colonies incubated with Cu-minerals, yet observations did not support this pathway. Combining our current and former experiments, we suggest that in natural settings the nutritional benefits gained by *Trichodesmium* via dust collection outweigh the risks of buoyancy loss and toxicity. Our data and concepts feed into the growing recognition of the significance of dust for *Trichodesmium*'s ecology and subsequently to ocean productivity.

Plain Language Summary

The abundant marine phytoplankton *Trichodesmium* spp. are nitrogen-fixing cyanobacteria that form extensive blooms in low latitude warm oceans and contribute significantly to carbon (C) and nitrogen (N) fixation, recycling and export. Desert dust deposited on the ocean surface is an important nutrient source for *Trichodesmium*. Spherical, millimeter-sized colonies of *Trichodesmium* from different ocean basins were reported to strongly interact with dust and shuffle dust particles to the colony core. While dust collection can optimize nutrient supply, it may come at a cost to *Trichodesmium*. Heavy dust loads may send the colonies to the deep ocean and metal release from dust may induce toxicity. Here, experimenting with Red Sea colonies and desert dust we studied some of the trade-offs of dust collection. Interacting colonies with dust, we examined the link between dust load and colony buoyancy. Combining dust dissolution measurements and mortality assays we examined toxicity thresholds for *Trichodesmium* surface blooms and dust-collecting colonies. We also studied the ability of colonies to remove particles and the effect of particle loss on their sinking velocity. Our experimental findings and concepts are valuable for assessing *Trichodesmium*'s distribution and ecophysiology and contribute to modeling of C or N transport to the deep ocean.

Key Points

- Dust collected by *Trichodesmium* colonies from seawater as a nutrient source may result in metal toxification and buoyancy loss.
- At moderate dust loads colonies maintained their buoyancy, but above a threshold sinking velocities increased linearly with dust loads.
- Desert dust induced *Trichodesmium* mortality through toxic metal release, but the lethal dose far exceeded oceanic dust concentrations.

1. Introduction

Trichodesmium spp. is a filamentous, N_2-fixing, and bloom-forming cyanobacterium inhabiting subtropical and tropical oligotrophic ocean regions and contributing ~40% of the annual global marine nitrogen fixation (Capone et al., 1997; Tang et al., 2020; Zehr & Capone, 2020). *Trichodesmium* spp. appear both as individual filaments (trichomes) and as colonies containing hundreds to thousands of trichomes organized in millimeter-sized tuft- or puff-shaped aggregates (Eichner et al., 2023). In the Red Sea, puff-shaped colonies are primarily composed of *Trichodesmium thiebautii* while tuft-shaped colonies are typically comprised of *Trichodesmium erythraeum* (Koedooder et al., 2022). The different colony morphologies also serve as micro-habitats for diverse microbes including bacteria, phytoplankton and even zooplankton, all exchanging nutrients and carbon throughout the colony life cycle from growth to demise (Anderson, 1977; Frischkorn et al., 2018; Lee et al., 2017; Rouco et al., 2016).

Natural *Trichodesmium* is often limited or co-limited by iron (Fe) and phosphorus (P) (Cerdan-Garcia et al., 2022; Held et al., 2020). Aerosol dust deposited on the ocean surface is considered an important nutrient source, but the low solubility of Fe and P minerals restricts its bioavailability for phytoplankton (Mills et al., 2004; Shaked et al., 2023; Shaked & Lis, 2012; Stockdale et al., 2016). Incubation studies revealed that *Trichodesmium* successfully grow on aerosol or dust (Chen et al., 2011; Polyviou et al., 2018) and even increase the bioavailability of dust Fe and P (Basu et al., 2019; Basu & Shaked, 2018; Shaked et al., 2023). An intriguing finding, which was reaffirmed in several studies is the ability of *Trichodesmium* colonies to actively collect and transport dust particles into the colony core (Kessler, Armoza-Zvuloni, et al., 2020; Rubin et al., 2011; Wang et al., 2022), which may serve to enhance dust dissolution, minimize nutrient loss by diffusion and optimize uptake (Eichner et al., 2023; Shaked et al., 2023). While these nutritional benefits are well established, yet studies exploring negative sides of particle collection to *Trichodesmium* remain scarce. Collection of heavy dust minerals may result in buoyancy loss and accelerate sinking to the deep ocean (Held et al., 2022; Pabortsava et al., 2017). Dust also contains an array of toxic elements (Bozlaker et al., 2013; Mackey et al., 2015), which upon gradual release within the colony core may induce toxicity and cause mortality. Our study focuses on this “dark side” of particle collection by, firstly, investigating the effect of dust on buoyancy and trace metal exposure of *Trichodesmium* and, secondly, examining active particle removal.

Depending on composition, dust particle density was reported to range from 2.1 to 2.6 g·cm^{-3} (McConnell et al., 2008; Schladitz et al., 2009), much denser than *Trichodesmium* with density of ~1 g·cm^{-3} (J. Kromkamp & Walsby, 1992; White et al., 2006). Consequently, collection of dust particles by *Trichodesmium* colonies increases their density and may affect *Trichodesmium*'s buoyancy. *Trichodesmium* spp. regulates its buoyancy through gas vesicles which can withstand high pressures (up to 12-37 bars, Walsby, 1992). This allows *Trichodesmium* to float on the water surface while also being able to resist hydraulic forces and conduct vertical migration to several hundred or thousand meters (Benavides et al., 2022; Pabortsava et al., 2017; Walsby, 1992). While a recent study modeled the effect of dust on sinking velocities of *Trichodesmium* (Held et al., 2022), experimental evidence linking dust loads and sinking velocities are missing.

Dust and other aerosols contain an array of elements, some of which are required as nutrients, while others such as cadmium (Cd), copper (Cu), lead (Pb) and arsenic (As) can be toxic (Guo et al., 2022; Mackey et al., 2012; Paytan et al., 2009; Yang et al., 2019). The potential toxicity of dust (or other aerosols) to *Trichodesmium* depends on the kinetics of toxic metal release to seawater, which in turn vary with aerosol types and sources, reactions occurring during atmospheric transport and particle to solvent ratios (Mackey et al., 2015; Mahowald et al., 2018; Stockdale et al., 2016). Natural populations of *Trichodesmium* colonies are reported to be very sensitive to toxic metals such as Cu and As (Hewson et al., 2009; Rueter et al., 1979). In addition to metals released from dust to the seawater surrounding natural *Trichodesmium*, the collection of dust within colonies further exposes them to toxic metals which gradually dissolve from the particles. However, dust toxicity to *Trichodesmium*, especially at the level of individual colonies, is poorly understood.

Our study focuses on this "dark side" of particle collection by investigating the effect of dust on buoyancy and trace metal exposure of *Trichodesmium* and examining active particle removal. These effects were investigated through two sets of experiments with natural *Trichodesmium* colonies: 1) sedimentation experiments with single colonies artificially loaded with dust, and 2) incubations with increasing dust concentrations probing mortality and metal release rates. The ability of *Trichodesmium* to mitigate these effects through particle removal was also examined. This research highlights potential trade-offs associated with particle collection and may contribute to predicting *Trichodesmium's* vertical distribution and role in C and N export to the deep ocean.

2. Material and methods

2.1 Colony & dust collection

Trichodesmium colonies were collected from the Gulf of Aqaba (29.56°N, 34.95°E) at the Northern Red Sea via net tows during 2018-2022. Each tow was conducted for ~7 min at the boat's minimal speed (1-2 knots) by deploying a 100 µm phytoplankton net (Aquatic Research Instrument, USA) to 10-20 m depth. The net concentrate was diluted into ~5 L seawater to minimize stress and well-shaped puff colonies were quickly hand-picked by droppers, placed in clean Petri dishes and washed three times with 0.22 µm filtered seawater (FSW). Dust samples were collected from the Gulf of Aqaba shores at the Inter-University Institute for Marine Sciences in Eilat (IUI). Samples of settled dust were collected from plastic surfaces located ~2 m from the sea, sieved through a 63 µm mesh, air-dried and stored in a desiccator.

2.2 Effect of dust load on colony buoyancy

Sedimentation experiments – During autumn 2020, sedimentation experiments were conducted on five consecutive days, on each testing five different colonies. Sinking velocities were measured in 18 cm tall sedimentation chambers (100 mL glass cylinders with 2.5 cm diameter). Colonies were gently introduced to chambers filled with fresh seawater and their vertical positions were recorded over time (see Fig. S1 for a schematic diagram and further details). Two types of data were collected: Initial colony sinking velocities in the chamber and colony positions in the chamber after 15 min. Each colony was tested three times: as is, and following interactions with medium and then high dust concentrations. All colonies were initially sinking and hence the sinking velocities were always positive. However, after 15 min colonies appeared to adjust their buoyancy and resumed different positions in the chamber. The ones at the bottom of the sedimentation chamber were defined as "sinkers" and the ones further up in the water as "floaters". Colony-dust interactions were induced by gently and repetitively mixing colonies within an eppendorf vial which contained seawater with the respective amount of dust. The dust load (weight) on each colony was calculated from stereoscopic images taken prior to introducing the colonies to the sedimentation chamber. Since many colonies lost dust particles during the experiments, another image was taken at the end of each experiment and dust weight was re-calculated.

Estimation of colony dust loads – Dust load (weight) was estimated from colony images taken with a stereoscope (Nikon, SMZ745). Using DinoCapture 2.0 and ImageJ software, the area of dust centered by the colony (μm^2) was estimated. This area was converted to volume (μm^3) assuming a constant thickness of 10 µm for the dust layer and then to mass using an average density of 2.5 $g \cdot cm^{-3}$ (see Fig. S2 for details; Kessler, Kraemer, et al., 2020). Similar analysis was done on published images of dust-containing colonies (Held et al., 2021).

Calculating the effect of dust on colony sinking velocities – Stoke's law and its modified equations has been widely applied in calculating and modeling sinking velocities of marine aggregates including natural *Trichodesmium* colonies (Jacco Kromkamp & Walsby, 1990; Laurenceau-Cornec et al., 2020; White et al., 2006). Recently, several attempts were made to assess the density change induced by internal ballasts (Benavides et al., 2022; Held et al., 2022). When colonies collect dust not only its mass needs to be considered but also its volume. To account for both, dust mass and volume, the Stoke's law-based equation, adapted for *Trichodesmium* by White et al. (2006), was modified (supplementary text S1). Based on this modified equation, the colony sinking velocity is predicted to increase linearly with dust load:

Equation. 1 Sinking velocity (dust-loaded colony) ($m \cdot d^{-1}$) =

Sinking velocity (dust-free colony) ($m \cdot d^{-1}$) + K ($m \cdot d^{-1} \cdot ng^{-1}$) x dust weight (ng)

The dust factor (K) is the velocity increase per dust mass with a unit of $m \cdot d^{-1} \cdot ng^{-1}$. Applying the measured colony size and the density of dust, Red Sea seawater and *Trichodesmium* cells (Basu & Shaked, 2018; Benaltabet et al., 2022; McConnell et al., 2008; Schladitz et al., 2009; White et al., 2006), we calculated that K=0.02-0.06 ($m \cdot d^{-1} \cdot ng^{-1}$) (supplementary text S2).

2.3 Metals in dust and toxicity to *Trichodesmium*

Dust dissolution experiments – Dust dissolution experiments were conducted in four separate experiments during 2015, using trace metal clean procedures, as described in Basu et al. (2019) and Gledhill et al. (2019). Local Red Sea dust was added to acid-cleaned Nalgene bottles containing gravimetrically quantified filtered seawater at final concentrations of 2 and 10 $mg \cdot L^{-1}$ and incubated at 25°C for 62 hours. 60 mL sub-samples were filtered through 0.22 µm syringe-filters (PVDF, Millex) using a Dynamax (Rainin) 8-head peristaltic pump under a clean bench. Sub-samples were stored for 6 months in trace metal cleaned high density polyethylene (HDPE) bottles and acidified to pH

~1.7 with ultra-clean HNO_3 prior to analysis of metals. Metals were analyzed by inductively coupled plasma mass spectrometry after preconcentration (SeaFAST pico) following the method of Rapp et al. (2017) and were quantified by standard addition (Krisch et al., 2022) at GEOMAR, Helmholtz Centre for Ocean Research, Kiel, Germany. Extending our experiments we also included dissolution measurements of local Red Sea dust samples from Mackey et al. (2015). We then split the dissolution data to two groups: 1) rapid dissolution (10 min and 6 h), and 2) gradual dissolution (1, 3 and 7 days).

Toxicity assays – Dust toxicity was investigated by incubating ~180 individual natural *Trichodesmium* colonies for 24 h in 48 well-plates with either dust suspension or dust leachate. Primary dust suspension was prepared daily in FSW and diluted to final concentrations of 2, 10, 100, 500, and 1000 $mg \cdot L^{-1}$. Dust leachates were obtained after 10 min by filtering the dust suspensions through 0.22 µm syringe-filters (PC membrane). Colonies were incubated in wells of a 48-well plate containing 0.5 mL dust suspension or leachate and were kept in a culture room (25 ^oC, ~80 $\mu E\ m^{-2}\ s^{-1}$, 10:14 h light-dark cycle). Visual changes of the colony and filament shape, structure, and color were monitored under a stereoscope at 2, 5, and 24 h (supplementary text S4). Incubations were repeated twice during spring 2022 and included controls without dust additions. Probing specifically for Cu toxicity, colonies were also incubated with dissolved Cu (5-3000 nM $CuSO_4$, supplementary text S4).

2.4 Removal of Cu-containing minerals

Hypothesizing that colonies may remove toxic minerals as a detoxification mechanism, 16 Red Sea colonies were incubated with the Cu mineral malachite ($Cu_2CO_3(OH)_2$). To ensure optimal colony-mineral interactions, malachite was mixed with hematite (α-Fe_2O_3), which is typically preferred by *Trichodesmium*. Individual colonies were sampled at different time points, placed on filters and probed for the presence of malachite via light microscopy and scanning electron microscopy with energy dispersive X-Ray analysis (SEM-EDX). Experiments were repeated for three days in autumn 2021. Malachite was obtained from Timna National Park (Eilat, Israel), crushed and sieved (<38µm), while hematite (<38µm) was obtained from the Mineral Collection at the National Natural History Collections at the Hebrew University of Jerusalem. Colonies were incubated in eppendorf vials under the IUI pier up to 24 hrs. At three time points, randomly selected colonies were imaged and placed on a PES membrane filter (Supor®), air-dried and frozen prior to SEM-EDX analysis (see supplementary text S5 for full details).

Microscopic SEM-EDX imaging – Colonies were placed on Supor® filters and coated with a ~10 nm carbon layer by thermal evaporation using a 108C Auto Carbon Coater (Ted Pella, Inc.) to avoid charging during the analysis. SEM images were collected with a FEI Helios NanoLab 600i field emission electron microscope. Specimen morphology was examined using a secondary electron Everhart-Thornley detector (ETD) in a field free mode at an acceleration voltage of 3 kV and a probe of 86 to 170 pA at 4 mm working distance. EDX analysis was performed at 10 to 20 kV and 1 to 2 nA with an X-Max 80mm^2 Silicon Drift Detector (SDD) from Oxford Instruments. Oxford AZtec software was used to collect compositional maps and point spectrum analyses.

3. Results and discussion

3.1 Dust loads and buoyancy control

Collection and centering of dust particles by *Trichodesmium* colonies may result in buoyancy loss and enhance their sinking velocities to the ocean depth. In the following section we present experimental results of natural colonies that were interacted with dust and tested in sedimentation chambers. The impact of dust on the colony buoyancy was examined by two different measures: 1) initial, short-term (~5 min) sinking velocity, and 2) colony position in the chamber after a 15 min acclimation period. All colonies had positive initial sinking velocities, but within 15 minutes some colonies left the chamber bottom and were re-suspended in the water. Colonies that remained on the bottom were considered as non-buoyant (“sinkers”), while those in the water were considered as buoyant (“floaters”).

3.1.1 How much dust can a colony bear to stay afloat?

At low dust loads (<100 ng) half of the colonies were classified as “floaters” (Fig. 1, orange symbols). At intermediate dust loads of 100-1000 ng, the fraction of “floaters” dropped but still accounted for ~30% of the colonies (Fig. 1, orange symbols). These findings demonstrate a remarkable ability of *Trichodesmium* to adjust their buoyancy to accommodate a significant dust load, assisted by their gas vesicles (Walsby, 1992). At increasing dust loads, and especially above 1 µg dust per colony, most colonies were defined as “sinkers” (Fig. 1, blue symbols), indicating a limit to *Trichodesmium*’s capacity to adapt its buoyancy.

Expanding the experimental data to natural conditions, dust loads associated with Red Sea *Trichodesmium* colonies collected from the upper 10-20 meters during 2018/19 were analyzed. These colonies were considered buoyant since they populated the upper water column and were plotted together with the experimentally determined “floaters” (Fig. 1a). Each colony typically contained 1-7 particles in sizes ranging between 10-70 µm in diameter (Table S1). The calculated weight of these particles amounted to 3-170 ng per colony and did not correlate with the colony volume (Fig. 1a, black crosses). These estimated dust-loads of floating, naturally occurring colonies, matched our experimental findings (Fig. 1a, orange circles). Similar weights of 200-300 ng dust per colony were also reported by Kessler et al. (2020), who analyzed SEM images of colonies collected from the upper 20 meters of the Gulf of Aqaba (Kessler, Kraemer, et al., 2020). Interestingly, the

Red Sea colonies fall short compared to Atlantic colonies collected from 20 m that remain afloat with much higher particle loads (Bif & Yunes, 2017; Held et al., 2021). Analyzing single colony images from the study of Held et al. (2021), we calculated dust loads of up to 10 µg per colony (Fig. 1a, green crosses). The ability to keep afloat with a higher dust load may stem from larger number of filaments in the colonies from the Atlantic compared with those from the Red Sea colonies. Based on these experiments and observations, we draw the threshold of dust that Red Sea puff-shaped colonies can bear and stay afloat at few hundred nanograms.

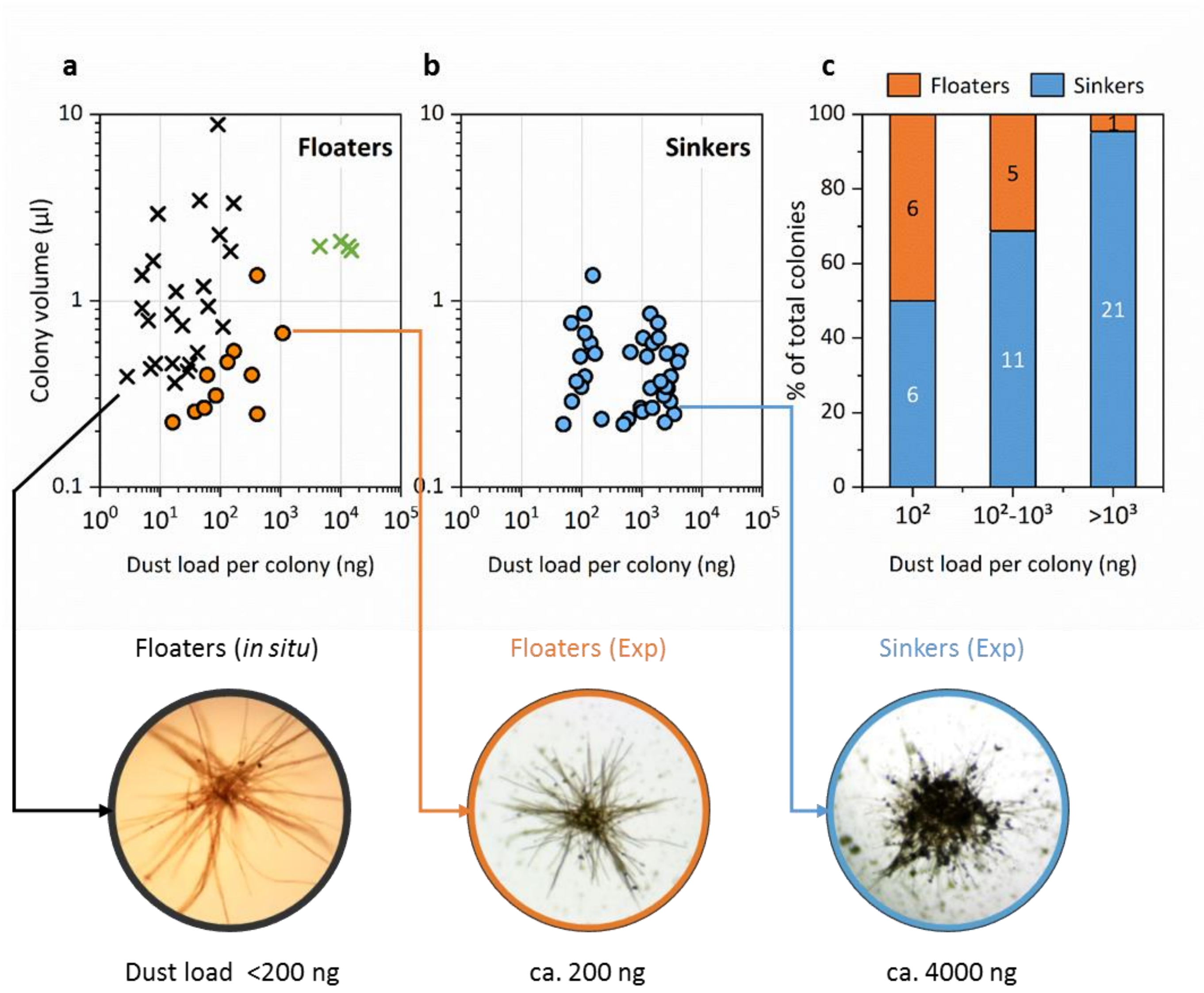

Figure 1. Effect of dust load on the buoyancy of natural *Trichodesmium* colonies.

Data compilation from natural colonies either containing particles when collected (crosses) or interacted with dust and tested in sedimentation experiments (circles). Colonies were categorized as “floaters” or “sinkers” according to their position in sedimentation chambers after 15 min. *In situ* colonies were defined as “floaters” since they were collected from the upper water column for 10-20 m depth.

(a) Range of dust loads associated with “floater” colonies tested in sedimentation experiments (n=12, orange circles) and freshly collected from the Red Sea (n=24, black crosses) and the Atlantic Ocean (n=4, green crosses, images from Held et al., 2021).

(b) Range of dust loads associated with “sinker” colonies tested in sedimentation experiments (n=38, blue circles).

(c) Fraction of experimentally determined “floaters” and “sinkers” as a function of dust load per colony. Pictures show typical dust loads as quantified through image analysis.

3.1.2 Effect of dust on colony sinking velocity

Initial sinking velocities for individual colonies were examined three times: without any dust, with medium dust load (20 to 1400 ng colony^{-1}), and with high dust load (330 to 4400 ng colony^{-1}). Experiments were repeated on five different days obtaining 75 data pairs of dust loads and sinking velocities (Table S2). As before, colonies were imaged prior to and after each step to track their actual dust loads. Data from two representative days (October 18th & 20th 2020) with six individual colonies show that moderate dust load of 100-400 ng did not affect the colony’s sinking velocity, which remained at 40-50 m·d^{-1} (Fig. 2a). The initial colony sinking velocities at these low dust loads were presumably controlled by colony size, colony composition (i.e. carbohydrate content) and gas vesicles but not by dust (Held et al., 2022; Walsby, 1992), a region which we term "colony-controlled" (Fig. 2, yellow area). This region is typified by the lack of effect of dust on the initial colony sinking velocity and is in-line with our other observations from the sedimentation chambers after 15 min (Fig. 1). Combined with field observations (Fig. 1a), our results suggest that Red Sea colonies can maintain their buoyancy when interacting with several hundred nanograms of dust.

Further dust addition (1-4 µg per colony) shifted the measured sinking velocities into a dust-controlled region (Fig 2, blue area). In this region, sinking velocities increased linearly with the colony’s dust load (Fig. 2b). A linear relationship is expected based on theoretical considerations (Stoke’s law) and direct sinking velocity measurements of size-specific ballasted aggregates (Engel et al., 2009; Iversen & Ploug, 2010). However, according to Stoke’s law, sinking velocity is impacted by both aggregate size and density (e.g. Laurenceau-Cornec et al., 2020). In our case, the colony size remained unchanged for all dust loads since it was centered within the colony core (as confirmed by microscopic observations). Taking into consideration the colony volume and density and the centered dust we derived a linear relationship between dust load and colony sinking velocity (Eq. 1), that should apply for the blue region (see methods and supplementary text S1 and S2). This theoretical calculation predicted a slope (K) of 0.02-0.06 m·d^{-1}·ng^{-1}, implying that 100 ng dust will increase the colony sinking velocity by 2-6 meters per day. Our experimental data yielded a slope (K) of 0.06 $m \cdot d^{-1} \cdot ng^{-1}$ (Fig. 2b) very similar to these theoretical predictions and thus supports our experimental approach. The match between experiments and predictions holds for dust-loaded colonies but not for dust-free colonies. Our measured sinking velocities of particle-free colonies (40-55 $m \cdot d^{-1}$, Fig. 2) exceed their predicted sinking velocities (0-9 $m \cdot d^{-1}$, Table S5). Yet, this mismatch may be explained by *Trichodesmium's* ability to modify their density (Romans et al., 1994; Tracy A. Villareal & Carpenter, 1990).

The sinking velocities measured (20-60 $m \cdot d^{-1}$) for particle-free colonies (Fig. 2) compare well with those of Walsby (1978), who experimentally observed maximal sinking velocities of 60 $m \cdot d^{-1}$ for natural *Trichodesmium thiebautii* from the Sargasso and Caribbean Sea. The vertical motion of *Trichodesmium* has been reported early-on (J. Kromkamp & Walsby, 1992; T. A. Villareal & Carpenter, 2003), and draws large interest in terms of carbon export to depth (Bonnet et al., 2023), and fueling of the deep ocean with fixed nitrogen (Benavides et al., 2022). Such vertical migration was hypothesized to provide an ecological advantage to *Trichodesmium* and enable it to mine phosphorus from the thermocline (Karl et al., 1992; White et al., 2006). Sinking of *Trichodesmium* colonies can occur through gravitational sinking or downwelling events (Guidi et al., 2012), both of which can further be accelerated by mineral ballasting (Pabortsava et al., 2017) or sudden autocatalytic cell death in response to nutrient limitation (Berman-Frank et al., 2004). Our study is the first to experimentally quantify the effect of dust on the colony's sinking velocity, and our findings conform to theoretical predictions, modelling data and *in situ* observations (Laurenceau-Cornec et al., 2020; Walsby, 1978; White et al., 2006). To conclude, our experiments show that *Trichodesmium* colonies can control their buoyancy even when loaded with up to 300-400 ng dust and that collection of 1 µg dust will slightly increase their sinking velocity by ~60 $m \cdot d^{-1}$.

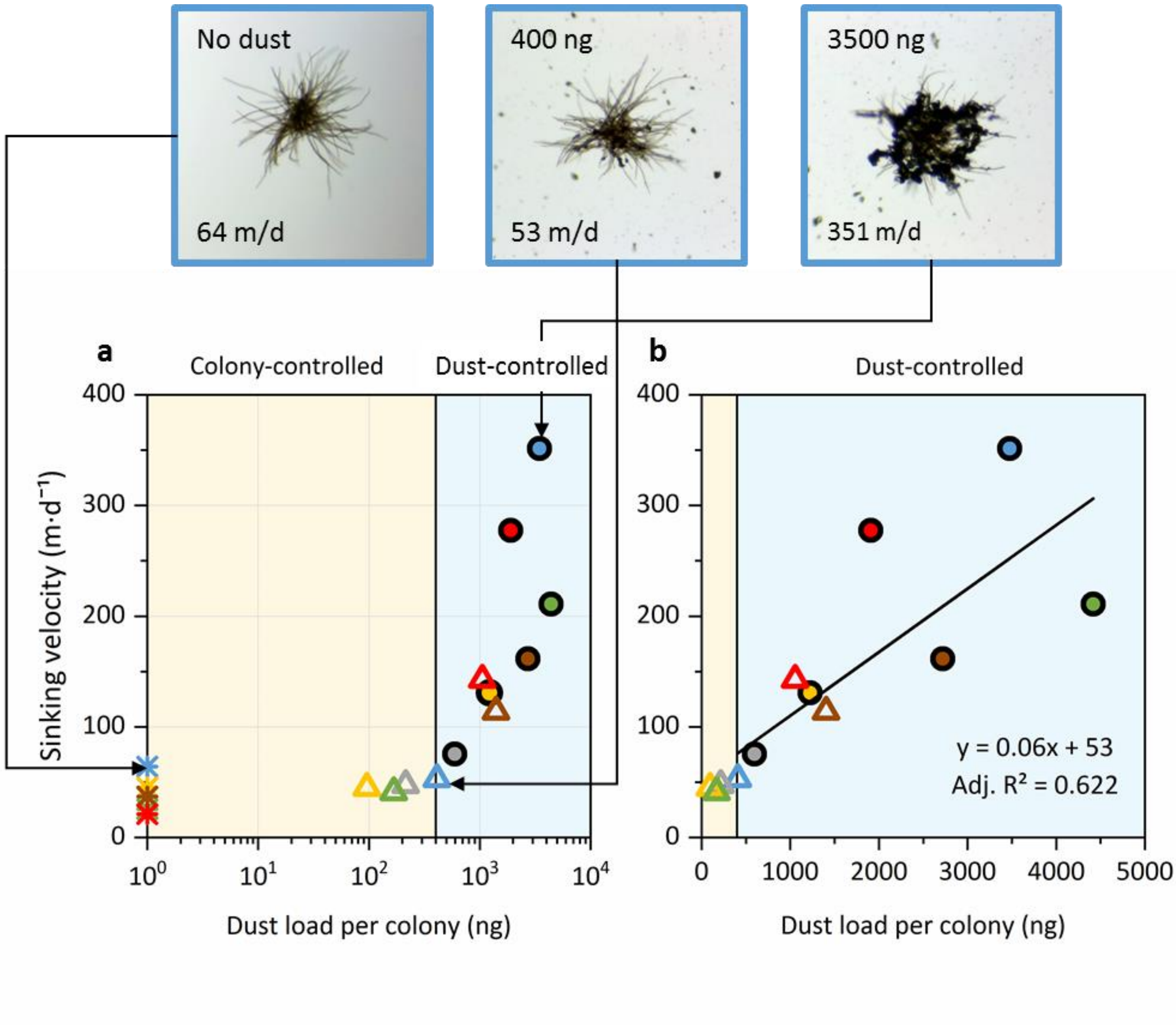

Figure 2. Effect of dust load on sinking velocities of Rea Sea *T. thiebautii* colonies.

(a) Sinking velocities of six individual colonies each measured repeatedly with increasing dust loads and labeled with a distinct color. Sinking velocities of particle-free colonies are noted by stars, colonies with medium dust load by triangles and colonies with high dust load by circles. Two regions were identified: colony-controlled area (yellow shaded) and dust-controlled area (blue shaded). Images above show the increasing dust loads of a single colony (blue-labeled).

(b) Zoom in on the dust-controlled zone, where sinking velocity increased linearly with dust load, at a slope (K) that matched theoretical calculations (see text).

3.1.3 Effect of dust loss on colony sinking velocity

During sedimentation experiments a significant loss of particles from most colonies (42 out of 50 total data pairs) was observed, especially from the heavily-loaded ones. Comparing colony images taken prior to and after the experiments, a loss of 10 ng - 3 µg dust per colony was calculated (Table S6). This massive loss of dust is expected to decrease the sinking velocity of colonies if the loss occurred in early stages of the experiment. Seeking to illustrate this effect, several representative colonies were plotted in Fig. 3 (see supplementary text S3 for the selection criterion) were compared to the linear relationship established in Fig. 2b (y = 0.06 $m \cdot d^{-1} \cdot ng^{-1}$ x dust weight (ng) + 53 $m \cdot d^{-1}$). All these colonies plot below their expected sinking velocities noted by the black line, indicating that dust was lost during the experiment and decreased their sinking velocities (Fig. 3a). Replotting the measured sinking velocities of these colonies against their final dust loads (Fig. 3b), yield values that are nearer to the line. Thus, it seems that these colonies were sinking at velocities that match the final dust loads, probably since this loss occurred at the beginning of the experiment. Such analysis, made possible by the relationship established in this study, revealed that dust loss can decrease the colony sinking velocity in a predictable manner.

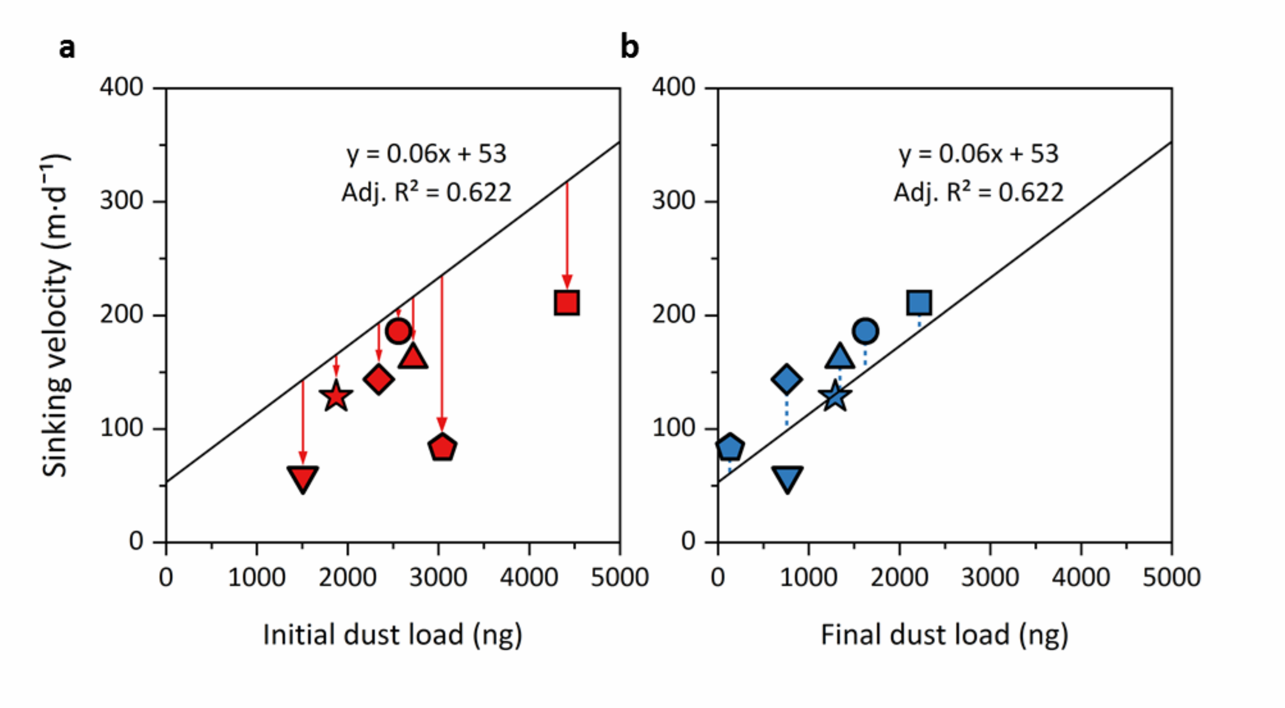

Figure 3. Effect of dust loss on colony sinking velocity.

Measured sinking velocities of seven representative colonies (shown as different symbols) plotted against their initial (a) and final (b) dust loads. The equation (black line) is the linear relationship established in Fig. 2b. Arrows and dash lines indicate the mismatch of measured sinking velocities and expected velocities calculated from initial and final dust loads, respectively. See Fig. S3 for additional colonies.

3.2 Toxic effects of dust on *Trichodesmium*

Dust and other aerosols contain an array of toxic elements (Bozlaker et al., 2013). Upon dust deposition on the surface ocean, some elements are rapidly released and may induce toxicity to positively buoyant *Trichodesmium* blooms that accumulate at the surface. Seeking to evaluate the toxicity of dust to *Trichodesmium* blooms, the fraction of rapidly released toxic metals was measured and the impact of dust leachate on *Trichodesmium* mortality was observed. In addition, colonies that concentrate dust may also experience a continuous flux of toxic metals that are gradually released from the centered particles. The gradual release of metals was hereby measured and the mortality of dust-loaded colonies was examined.

3.2.1 Kinetics of toxic metal release from dust

Toxic metal release to seawater was measured at two dust concentrations and data was gathered according to time, differentiating between rapidly (10 min - 6 h) and gradually (12 h - 7 d) released elements. To contextualize our data, we included additional dissolution measurements conducted by Mackay et al. (2015) resulting in a dissolution dataset composed of seven different dust samples collected from the Gulf of Aqaba over several years (Fig. 4, see Table S7 for additional elements). To enable easy extrapolation to natural conditions, concentrations of dissolved metal released from the different dust samples were plotted against the concentrations of dust used in the experiments. In general, higher dissolved metals were recorded at higher dust concentrations and a linear correlation can be fitted to the data (Fig. 4).

Since *Trichodesmium's* exposure to dust depends on the interaction time, special attention was paid to the timing and release mode of each metal, following the Mackay et al. (2015) scheme. Concentrations of zinc (Zn) and cadmium (Cd) remained constant with time (gradual=rapid, Fig. 4) and hence were considered rapidly released elements. On the other hand, aluminum (Al) and copper (Cu) accumulated with dissolution time (gradual>rapid, Fig. 4), and were considered gradually released elements. Lead (Pb) concentration dropped slightly with time (gradual<rapid, Fig. 4), reflecting its tendency to adsorb onto particles and surfaces (Bruland et al., 2013). Based on these linear slopes and release mode (rapid versus gradual), the "cocktail" of toxic elements released during dust deposition events or within the colony center can be evaluated and linked to the incubation studies with *Trichodesmium*.

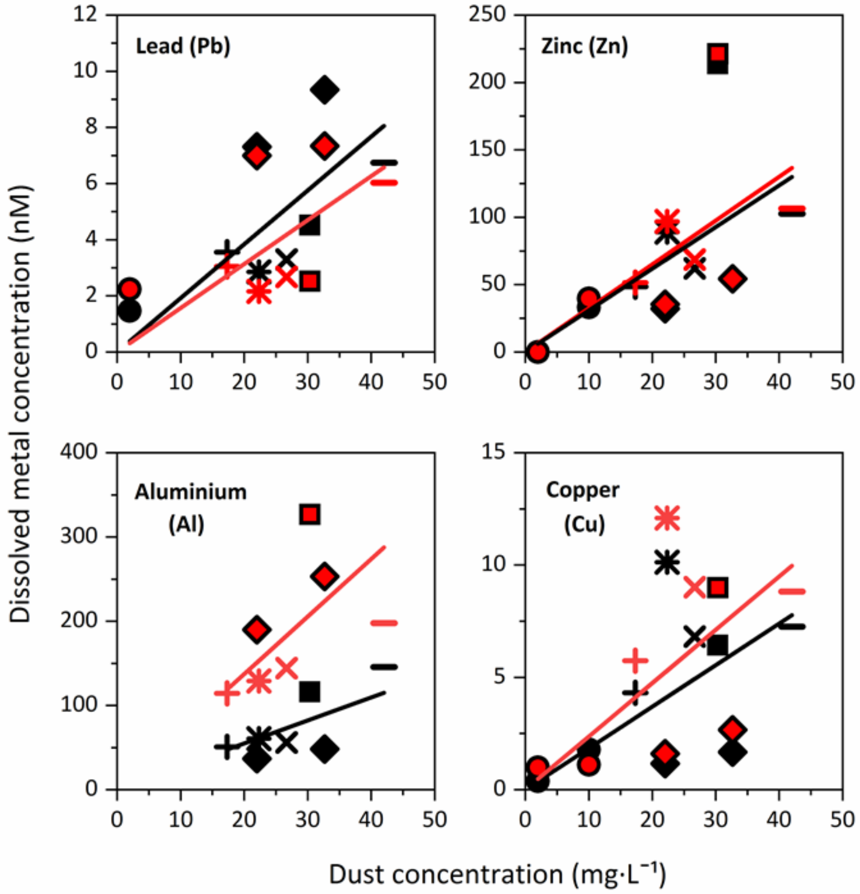

Toxic metal	Regression slopes Rapid diss.	Regression slopes Gradual diss.
	nmol · (mg dust)$^{-1}$	nmol · (mg dust)$^{-1}$
Pb	0.19	0.16
Zn	3.09	3.25
Cd	0.01	0.01
Al	2.74	6.85
Cu	0.18	0.24

Figure 4. Compilation of dust dissolution experiments conducted in seawater using different dust samples and concentrations.

The dataset combines new measurements (circles) and published data from (Mackey et al., 2015) and includes seven dust samples plotted as different symbols. Metal release kinetics is presented by two categories - rapidly released metals (black, up to 6hrs) and gradually released metals (red, up to 7 days). Regression slopes linking dust and dissolved metal concentrations are plotted and summarized in the table next to the graph (see Fig. S6 for additional elements).

3.2.2 Dust toxicity to Trichodesmium – fractions and doses

To assess dust toxicity to *Trichodesmium*, ~180 freshly collected natural colonies were incubated with increasing dust concentrations for 24 hrs and mortality was assessed visually based on colony integrity and filament degradation (Fig. S4). To distinguish between the toxic effects of rapidly and gradually released metals, colonies were exposed to dust leachate and raw dust, respectively (where the leachate was obtained after 10 min from dust addition to seawater).

Incubating *Trichodesmium* with 2 and 10 $mg \cdot L^{-1}$ dust resulted in negligible mortality of only one or two of the 16 colonies incubated (red and blue lines in Fig. 5a and 5b). These dust loads are within the range reported for natural dust storms (<10 $mg \cdot L^{-1}$, Ren et al., 2011; Zhang et al., 2019), and hence dust load from such storms are not predicted to induce *Trichodesmium* mortality. Low mortality (13%) was observed in colonies incubated with 100 $mg \cdot L^{-1}$ dust leachate, far below the LC50 toxicity threshold, which is the lethal concentration that results in death of 50% of the colonies (Echeveste et al., 2012). At higher dust concentrations of 500 and 1000 $mg \cdot L^{-1}$, significant mortality was observed, ranging from 50-90% of the colonies (purple and orange lines in Fig. 5a and Fig. 5b), indicative of acute toxicity. Based on these incubations, we conservatively set the LC50 toxicity threshold at 500 $mg \cdot L^{-1}$ (although it may occur anywhere above 100 $mg \cdot L^{-1}$).

Overall, the mortality of *Trichodesmium* was comparable between the leachate (Fig. 5a) and dust particles (Fig. 5b). This implies that metals released from dust during 10 min are the key contributors to its toxicity to *Trichodesmium*. Utilizing the linear fit from Fig. 4, toxic metals concentrations in each incubation can be estimated (Fig. 5c). For example, in the incubation with 500 $mg \cdot L^{-1}$ dust that yielded 50% mortality, *Trichodesmium* is expected to experience 5 nM Cd, 95 nM Pb, 90 nM Cu, and >1 μM of Zn and Al (Fig. 5c). Interestingly, negligible mortality occurred in the 100 $mg \cdot L^{-1}$ dust leachate incubation, conditions where 1 nM Cd, ~20 nM Pb and Cu, and ~300 nM of Zn and Al were predicted (Fig. 5b and 5c). Given the absence of literature data on *Trichodesmium*'s response to a cocktail of toxic metals, it remains inconclusive whether these levels were sub-lethal or *Trichodesmium* was capable of detoxifying these metals. Typically, toxicity thresholds (e.g. effective concentration 50% (EC50s) or lethal concentration 50% (LC50s) are obtained for a single metal, varying amongst phytoplankton types and sizes (Echeveste et al., 2012; Paytan et al., 2009; Yang et al., 2019). To provide context, Cd and Pb toxicity thresholds (LC50s) for natural phytoplankton from different ocean basins were reported to range from 2-4000 nM for Cd, and 100-2000 nM for Pb (Echeveste et al., 2012).

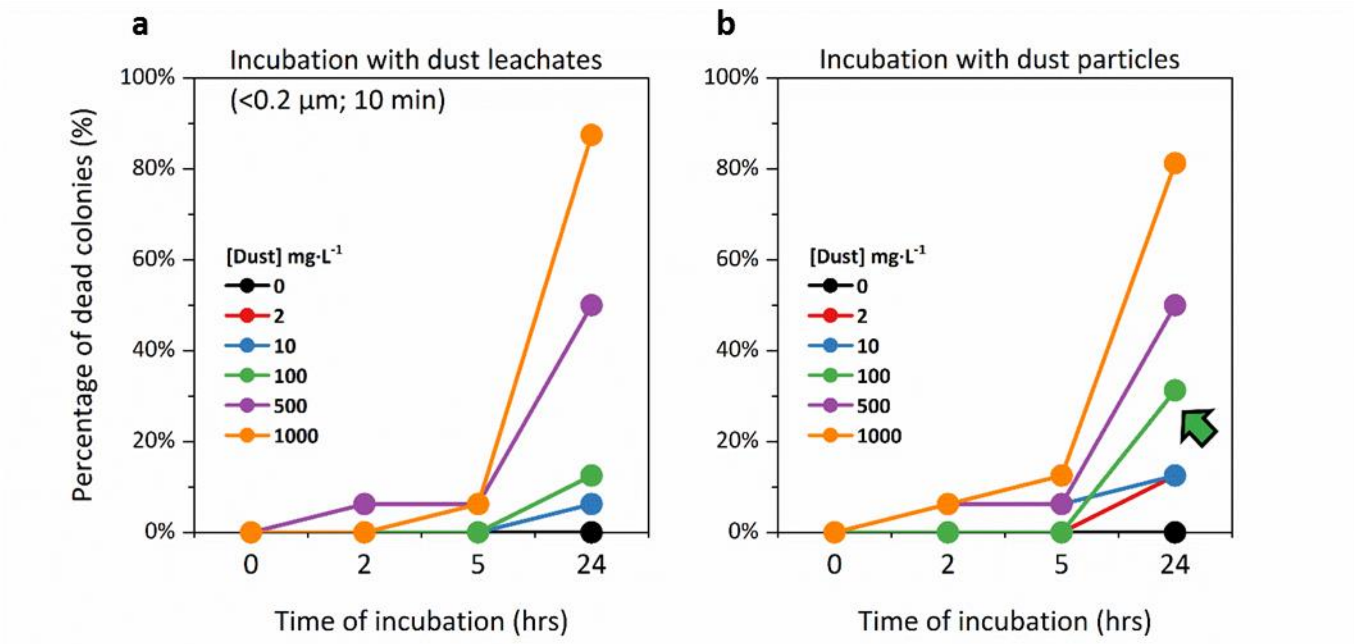

c Calculated toxic metal release from dust

Dust concn. (mg·L^{-1})	Rapid release in dust-leachates (nM)					Gradual release (nM)	
	Pb	Zn	Cd	Al	Cu	Al*	Cu*
1000	190	3090	10	2740	180	4110	60
500	95	1545	5	1370	90	2055	30
100	19	309	1	274	18	411	6
10	1.9	31	0.1	27	1.8	41	0.6
2	0.4	6	0.0	5	0.4	8	0.1

* represents additional release during incubation

Figure 5. Impact of dust on mortality of Red Sea *Trichodesmium* colonies and estimated toxic metals released during incubations.

Mortality of natural colonies incubated for 24 hrs with increasing concentrations of (a) dust leachate and (b) whole dust. (c). Calculated metal release from dust during the mortality assays based on the regression slopes obtained in Fig. 4. Data was compiled from 2 different experiments. The dust leachate was filtered within 10 min of dust suspension in seawater to represent rapidly released metals, while whole dust provided also gradually released metals. The toxicity of dust leachate and whole dust was comparable at high concentrations, but as indicated by the green arrow, at 100 mg·L^{-1} dust, the mortality was higher with whole dust.

A more detailed look at the data shows subtle changes in the mortality of colonies incubated with 100 mg·L^{-1} dust leachate compared to the whole dust (green arrow in Fig. 5). At these low dust concentrations (e.g. 100 mg·L^{-1}), only two colonies died in the leachate (13%), while five colonies died in the whole dust (31%). This added mortality may have originated from the gradually released metals Al and Cu (Fig. 5c). In a parallel set of experiments, we tested the mortality of colonies incubated with increasing Cu concentrations, obtaining 30 and 50% mortality at 5 and 10 nM Cu, respectively (Fig. S5). The estimated gradually release of 0.1-6 nM Cu (Fig. 5c) may hereby explain the elevated mortality in the whole dust incubation, especially when also considering the high levels of Al.

Regarding the toxicity of metals in dust-centering colonies, it appears that Pb, Zn and Cd are not a major concern, as these elements are released from dust before they interact with the colonies. But the gradually released elements Al and Cu may cause toxicity to colonies that center dust. As dust is confined within the colony core and the diffusion to the surrounding water is limited, the colony or its core volume should be considered as the relevant volume for metal release. Given ~1 µL colony volume, dust loads of 0.2-1 µg yield effective dust concentration of 200-1000 mg·L^{-1} (Fig. S7). At these high dust concentrations, high exposure to gradually released Al and Cu is expected (Fig. 5c). The exposure to these metals may be even larger when considering the volume of the colony core where the dissolution occurs and not the entire colony volume. Nonetheless, colonies that accumulated even higher dust loads (1-10 µg) showed no signs of mortality during incubations that lasted 24 hrs (Fig. S8). The survival of colonies with an effective dust load of over 1000 mg·L^{-1} and projected high Cu and Al fluxes (Fig. 5c) is intriguing. These observations call for further research measuring metal fluxes within colonies and exploring possible detoxification and physiological defense mechanisms. Such mechanisms may include metal binding by extracellular polymeric substances (EPS) and specific ligands (Gledhill et al., 2019) and metal excretion through efflux proteins (Hewson et al., 2009).

3.2.3 Selective removal of Cu minerals

Hypothesizing that colonies may try to reduce toxicity through the removal of particles, natural colonies were incubated with Cu-containing minerals (malachite) for 24 hrs. To ensure optimal colony-mineral interactions, the Cu minerals were mixed with Fe minerals (hematite), which are typically preferred by *Trichodesmium*. All colonies interacted strongly with particles throughout the incubation and showed strong preference for the Fe-minerals. Only few colonies contained Cu-minerals, but these were present even at 24 hrs (Fig. 6). The finding of Cu minerals on colonies at the end of the incubation does not support our hypothesis and there is currently no evidence to support the selective removal of toxic minerals.

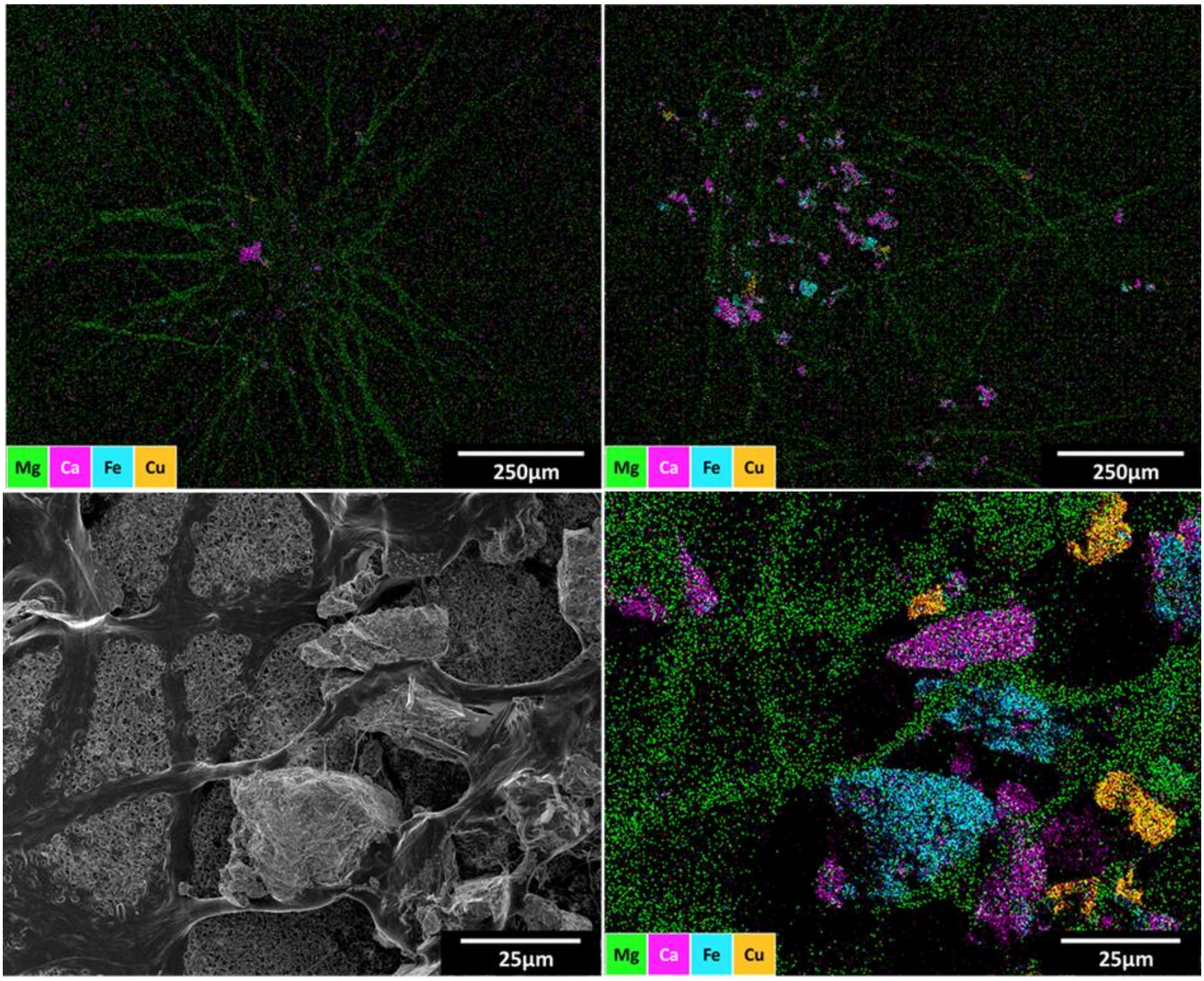

Figure 6. SEM-EDX images of natural *Trichodesmium* colonies incubated with Cu-minerals (malachite) and Fe-minerals (hematite).

Probing the ability of *Trichodesmium* to distinguish and selectively remove toxic particles, colonies were incubated with malachite and hematite up to 24 hrs. Several colonies were imaged at different magnification (scale bars within images), showing the presence of both minerals throughout the incubation (Cu – yellow, Fe – blue). *Trichodesmium* was imaged through its magnesium content (green) and the malachite sample also contained calcium (Ca) minerals (pink). See Fig. S10-S13 for additional elemental maps.

4. Summary

Having studied the potential negative effects of dust on natural *Trichodesmium* colonies, we predict that in a typical open-ocean setting, the potential benefit of dust as a nutrient source outweighs the risks of buoyancy loss and toxification. In the Gulf of Aqaba, puff-shaped *T. thiebautii* colonies collected *in situ* were usually observed to contain less than 200 ng of dust per colony, which is below the threshold where sinking velocity becomes dust-controlled (Fig. 1) and is insufficient to induce toxicity through metal release (Fig. 5). In other environments (e.g. coastal seas, Mackey et al., 2012), however, *Trichodesmium* may encounter more toxic aerosols and the concepts laid here may facilitate the evaluation of those risks. With regards to buoyancy, accelerated sinking velocities due to interactions with dust may be significant to C export, and may help explain recent measurements of active N_2 fixation by *Trichodesmium* at 1000 meters (Benavides et al., 2022). If indeed colonies can modulate their particle load, the dust-induced sinking may benefit *Trichodesmium* and expand its ecological niche.

Author contributions

Conceptualization: Siyuan Wang, Yeala Shaked

Data curation: Siyuan Wang

Formal analysis: Siyuan Wang, Futing Zhang, Coco Koedooder, Odeta Qafoku, Subhajit Basu, Stephan Krisch, Anna-Neva Visser, Meri Eichner, Nivi Kessler

Methodology: Siyuan Wang, Futing Zhang, Odeta Qafoku, Subhajit Basu, Stephan Krisch, Anna-Neva Visser

Funding acquisition: Rene M. Boiteau, Martha Gledhill, Yeala Shaked

Supervision: Yeala Shaked

Writing – original draft: Siyuan Wang, Yeala Shaked

Writing – review & editing: Futing Zhang, Coco Koedooder, Odeta Qafoku, Subhajit Basu, Stephan Krisch, Anna-Neva Visser, Meri Eichner, Nivi Kessler, Rene M. Boiteau, Martha Gledhill

Acknowledgements

We extend our sincere gratitude to Murielle Dray (IUI) and Emanuel Sestieri (IUI) for their invaluable assistance during this study. We appreciate the Mineral collection at the National Natural History Collections at the Hebrew University for donating the mineral specimens (hematite) used in this work. Siyuan Wang thanks Prof. Angelicque E. White for her insightful suggestions regarding the model of sinking velocity and to Mr. Antonio Colussi and Dr. Lina Sakhneny for their contributions to colony collection and toxicity assays. This study was funded by ISF-NSFC joint research program (Grant No. 2398/18) and ISF (260/21). Siyuan Wang acknowledges CSC-HUJI doctoral fellowship and Futing Zhang acknowledges PBC Postdoctoral fellowship.

Conflict of interest

The authors declare that they have no conflict of interest.

Data availability statement

Data generated for this study were uploaded as supplementary materials. All python codes for sinking velocity can be found in Github (*https://github.com/Zhanzhu1110/Trichobuoyancy.git*) and in Zenodo (*https://zenodo.org/records/10290901*; DOI:10.5281/zenodo.10290901)(Wang et al., 2023). Data of metal release (dust concentrations = 17-42 mg·L^{-1}) are available from Mackay et al. (2015), and a complete supplementary data file is also provided herein for ease of access.

Reference

Anderson, O. R. (1977). Fine Structure of a Marine Ameba Associated with a Blue-Green Alga in the Sargasso Sea. *The Journal of Protozoology*, *24*(3), 370–376. https://doi.org/10.1017/cbo9780511600586.003

Basu, S., & Shaked, Y. (2018). Mineral iron utilization by natural and cultured *Trichodesmium* and associated bacteria. *Limnology and Oceanography*, *63*(6), 2307–2320. https://doi.org/10.1002/lno.10939

Basu, S., Gledhill, M., de Beer, D., Prabhu Matondkar, S. G., & Shaked, Y. (2019). Colonies of marine cyanobacteria *Trichodesmium* interact with associated bacteria to acquire iron from dust. *Communications Biology*, *2*(1), 1–8. https://doi.org/10.1038/s42003-019-0534-z

Benaltabet, T., Lapid, G., & Torfstein, A. (2022). Dissolved aluminium dynamics in response to dust storms, wet deposition, and sediment resuspension in the Gulf of Aqaba, northern Red Sea. *Geochimica et Cosmochimica Acta*, *335*, 137–154. https://doi.org/10.1016/j.gca.2022.08.029

Benavides, M., Bonnet, S., Le Moigne, F. A. C., Armin, G., Inomura, K., Hallstrøm, S., et al. (2022). Sinking *Trichodesmium* fixes nitrogen in the dark ocean. *ISME Journal*, *16*(10), 2398–2405. https://doi.org/10.1038/s41396-022-01289-6

Berman-Frank, I., Bidle, K. D., Haramaty, L., & Falkowski, P. G. (2004). The demise of the marine cyanobacterium, *Trichodesmium* spp., via an autocatalyzed cell death pathway. *Limnology and Oceanography*, *49*(4 I), 997–1005. https://doi.org/10.4319/lo.2004.49.4.0997

Bif, M. B., & Yunes, J. S. (2017). Distribution of the marine cyanobacteria *Trichodesmium* and their association with iron-rich particles in the South Atlantic Ocean. *Aquatic Microbial Ecology*, *78*(2), 107–119. https://doi.org/10.3354/ame01810

Bonnet, S., Benavides, M., Le Moigne, F. A. C., Camps, M., Torremocha, A., Grosso, O., et al. (2023). Diazotrophs are overlooked contributors to carbon and nitrogen export to the deep ocean. *ISME Journal*, *17*(1), 47–58. https://doi.org/10.1038/s41396-022-01319-3

Bozlaker, A., Prospero, J. M., Fraser, M. P., & Chellam, S. (2013). Quantifying the contribution of long-range saharan dust transport on particulate matter concentrations in Houston, Texas, using detailed elemental analysis. *Environmental Science and Technology*, *47*(18), 10179–10187. https://doi.org/10.1021/es4015663

Bruland, K. W., Middag, R., & Lohan, M. C. (2013). *Controls of Trace Metals in Seawater*. *Treatise on Geochemistry: Second Edition* (2nd ed., Vol. 8). Elsevier Ltd. https://doi.org/10.1016/B978-0-08-095975-7.00602-1

Capone, D. G., Zehr, J. P., Paerl, H. W., Bergman, B., & Carpenter, E. J. (1997). *Trichodesmium*, a globally significant marine cyanobacterium. *Science*, *276*(5316), 1221–1229. https://doi.org/10.1126/science.276.5316.1221

Cerdan-Garcia, E., Baylay, A., Polyviou, D., Woodward, E. M. S., Wrightson, L., Mahaffey, C., et al. (2022). Transcriptional responses of *Trichodesmium* to natural inverse gradients of Fe and P availability. *ISME Journal*, *16*(4), 1055–1064. https://doi.org/10.1038/s41396-021-01151-1

Chen, Y., Tovar-Sanchez, A., Siefert, R. L., Sañudo-Wilhelmy, S. A., & Zhuang, G. (2011). Luxury uptake of aerosol iron by *Trichodesmium* in the western tropical North Atlantic. *Geophysical Research Letters*, *38*(18). https://doi.org/10.1029/2011GL048972

Echeveste, P., Agustí, S., & Tovar-Sánchez, A. (2012). Toxic thresholds of cadmium and lead to oceanic phytoplankton: Cell size and ocean basin-dependent effects. *Environmental Toxicology and Chemistry*, *31*(8), 1887–1894. https://doi.org/10.1002/etc.1893

Eichner, M., Inomura, K., Pierella Karlusich, J. J., & Shaked, Y. (2023). Better together? Lessons on sociality from *Trichodesmium*. *Trends in Microbiology*, *xx*(xx), 1–13. https://doi.org/10.1016/j.tim.2023.05.001

Engel, A., Szlosek, J., Abramson, L., Liu, Z., & Lee, C. (2009). Investigating the effect of ballasting by $CaCO_3$ in Emiliania huxleyi: I. Formation, settling velocities and physical properties of aggregates. *Deep-Sea Research Part II: Topical Studies in Oceanography*, *56*(18), 1396–1407. https://doi.org/10.1016/j.dsr2.2008.11.027

Frischkorn, K. R., Haley, S. T., & Dyhrman, S. T. (2018). Coordinated gene expression between *Trichodesmium* and its microbiome over day-night cycles in the North Pacific Subtropical Gyre. *ISME Journal*, *12*(4), 997–1007. https://doi.org/10.1038/s41396-017-0041-5

Gledhill, M., Basu, S., & Shaked, Y. (2019). Metallophores associated with: *Trichodesmium* erythraeum colonies from the Gulf of Aqaba. *Metallomics*, *11*(9), 1547–1557. https://doi.org/10.1039/c9mt00121b

Guidi, L., Calil, P. H. R., Duhamel, S., Björkman, K. M., Doney, S. C., Jackson, G. A., et al. (2012). Does eddy-eddy interaction control surface phytoplankton distribution and carbon export in the North Pacific Subtropical Gyre? *Journal of Geophysical Research: Biogeosciences*, *117*(2), 1–12. https://doi.org/10.1029/2012JG001984

Guo, C., Zhou, Y., Zhou, H., Su, C., & Kong, L. (2022). Aerosol Nutrients and Their Biological Influence on the Northwest Pacific Ocean (NWPO) and Its Marginal Seas. *Biology*, *11*(6), 1–18. https://doi.org/10.3390/biology11060842

Held, N. A., Webb, E. A., McIlvin, M. M., Hutchins, D. A., Cohen, N. R., Moran, D. M., et al. (2020). Co-occurrence of Fe and P stress in natural populations of the marine diazotroph *Trichodesmium*. *Biogeosciences*, *17*(9), 2537–2551. https://doi.org/10.5194/bg-17-2537-2020

Held, N. A., Sutherland, K. M., Webb, E. A., McIlvin, M. R., Cohen, N. R., Devaux, A. J., et al. (2021). Mechanisms and heterogeneity of *in situ* mineral processing by the marine nitrogen fixer *Trichodesmium* revealed by single-colony metaproteomics. *ISME Communications*, *1*(1), 1–9. https://doi.org/10.1038/s43705-021-00034-y

Held, N. A., Waterbury, J. B., Webb, E. A., Kellogg, R. M., McIlvin, M. R., Jakuba, M., et al. (2022). Dynamic diel proteome and daytime nitrogenase activity supports buoyancy in the cyanobacterium *Trichodesmium*. *Nature Microbiology*, *7*(2), 300–311. https://doi.org/10.1038/s41564-021-01028-1

Hewson, I., Poretsky, R. S., Dyhrman, S. T., Zielinski, B., White, A. E., Tripp, H. J., et al. (2009). Microbial community gene expression within colonies of the diazotroph, *Trichodesmium*, from the Southwest Pacific Ocean. *ISME Journal*, *3*(11), 1286–1300. https://doi.org/10.1038/ismej.2009.75

Iversen, M. H., & Ploug, H. (2010). Ballast minerals and the sinking carbon flux in the ocean: Carbon-specific respiration rates and sinking velocity of marine snow aggregates. *Biogeosciences*, *7*(9), 2613–2624. https://doi.org/10.5194/bg-7-2613-2010

Karl, D. M., Letelier, R., Hebel, D. V., Bird, D. F., & Winn, C. D. (1992). *Trichodesmium* blooms and new nitrogen in the North Pacific gyre. In J. G. Carpenter, E.J., Capone, D.G., Rueter (Ed.), *Marine pelagic cyanobacteria* (pp. 219–237). Springer, Dordrecht. https://doi.org/10.1007/978-94-015-7977-3_14

Kessler, N., Kraemer, S. M., Shaked, Y., & Schenkeveld, W. D. C. (2020). Investigation of Siderophore-Promoted and Reductive Dissolution of Dust in Marine Microenvironments Such as *Trichodesmium* Colonies. *Frontiers in Marine Science*, *7*(March), 1–15. https://doi.org/10.3389/fmars.2020.00045

Kessler, N., Armoza-Zvuloni, R., Wang, S., Basu, S., Weber, P. K., Stuart, R. K., & Shaked, Y. (2020). Selective collection of iron-rich dust particles by natural *Trichodesmium* colonies. *ISME Journal*, *14*(1), 91–103. https://doi.org/10.1038/s41396-019-0505-x

Koedooder, C., Landou, E., Zhang, F., Wang, S., Basu, S., Berman-Frank, I., et al. (2022). Metagenomes of Red Sea Subpopulations Challenge the Use of Marker Genes and Morphology to Assess *Trichodesmium* Diversity. *Frontiers in Microbiology*, *13*(May). https://doi.org/10.3389/fmicb.2022.879970

Krisch, S., Hopwood, M. J., Roig, S., Gerringa, L. J. A., Middag, R., Rutgers van der Loeff, M. M., et al. (2022). Arctic – Atlantic Exchange of the Dissolved Micronutrients Iron, Manganese, Cobalt, Nickel, Copper and Zinc With a Focus on Fram Strait. *Global Biogeochemical Cycles*, *36*(5). https://doi.org/10.1029/2021GB007191

Kromkamp, J., & Walsby, A. E. (1992). Buoyancy regulation and vertical migration of *Trichodesmium*: a computer-model prediction. In J. G. Carpenter, E.J., Capone, D.G., Rueter (Ed.), *Marine Pelagic Cyanobacteria: Trichodesmium and other Diazotrophs* (pp. 239–248). Springer, Dordrecht. https://doi.org/10.1007/978-94-015-7977-3_15

Kromkamp, Jacco, & Walsby, A. E. (1990). A computer model of buoyancy and vertical migration in cyanobacteria. *Journal of Plankton Research*, *12*(1), 161–183. https://doi.org/10.1093/plankt/12.1.161

Laurenceau-Cornec, E. C., Le Moigne, F. A. C., Gallinari, M., Moriceau, B., Toullec, J., Iversen, M. H., et al. (2020). New guidelines for the application of Stokes' models to the sinking velocity of marine aggregates. *Limnology and Oceanography*, *65*(6), 1264–1285. https://doi.org/10.1002/lno.11388

Lee, M. D., Walworth, N. G., McParland, E. L., Fu, F. X., Mincer, T. J., Levine, N. M., et al. (2017). The *Trichodesmium* consortium: Conserved heterotrophic co-occurrence and genomic signatures of potential interactions. *ISME Journal*, *11*(8), 1813–1824. https://doi.org/10.1038/ismej.2017.49

Mackey, K. R. M., Buck, K. N., Casey, J. R., Cid, A., Lomas, M. W., Sohrin, Y., & Paytan, A. (2012). Phytoplankton responses to atmospheric metal deposition in the coastal and open-ocean Sargasso Sea. *Frontiers in Microbiology*, *3*(OCT), 1–15. https://doi.org/10.3389/fmicb.2012.00359

Mackey, K. R. M., Chien, C. Te, Post, A. F., Saito, M. A., & Paytan, A. (2015). Rapid and gradual modes of aerosol trace metal dissolution in seawater. *Frontiers in Microbiology*, *6*(JAN), 1–11. https://doi.org/10.3389/fmicb.2014.00794

Mahowald, N. M., Hamilton, D. S., Mackey, K. R. M., Moore, J. K., Baker, A. R., Scanza, R. A., & Zhang, Y. (2018). Aerosol trace metal leaching and impacts on marine microorganisms. *Nature Communications*, *9*(1). https://doi.org/10.1038/s41467-018-04970-7

McConnell, C. L., Highwood, E. J., Coe, H., Formenti, P., Anderson, B., Osborne, S., et al. (2008). Seasonal variations of the physical and optical characteristics of saharan dust: Results from the dust outflow and deposition to the ocean (DODO) experiment. *Journal of Geophysical Research*, *113*, 1–19. https://doi.org/10.1029/2007JD009606

Mills, M. M., Ridame, C., Davey, M., La Roche, J., & Geider, R. J. (2004). Iron and phosphorus co-limit nitrogen fixation in the eastern tropical North Atlantic. *Nature*, *429*(6989), 292–294. https://doi.org/10.1038/nature03632

Pabortsava, K., Lampitt, R. S., Benson, J., Crowe, C., McLachlan, R., Le Moigne, F. A. C., et al. (2017). Carbon sequestration in the deep Atlantic enhanced by Saharan dust. *Nature Geoscience*, *10*(3), 189–194. https://doi.org/10.1038/ngeo2899

Paytan, A., Mackey, K. R. M., Chen, Y., Lima, I. D., Doney, S. C., Mahowald, N., et al. (2009). Toxicity of atmospheric aerosols on marine phytoplankton. *Proceedings of the National Academy of*

Sciences of the United States of America, *106*(12), 4601–4605. https://doi.org/10.1073/pnas.0811486106

Polyviou, D., Baylay, A. J., Hitchcock, A., Robidart, J., Moore, C. M., & Bibby, T. S. (2018). Desert dust as a source of iron to the globally important diazotroph *Trichodesmium*. *Frontiers in Microbiology*, *8*(JAN), 1–12. https://doi.org/10.3389/fmicb.2017.02683

Rapp, I., Schlosser, C., Rusiecka, D., Gledhill, M., & Achterberg, E. P. (2017). Automated preconcentration of Fe, Zn, Cu, Ni, Cd, Pb, Co, and Mn in seawater with analysis using high-resolution sector field inductively-coupled plasma mass spectrometry. *Analytica Chimica Acta*, *976*, 1–13. https://doi.org/10.1016/j.aca.2017.05.008

Ren, J. L., Zhang, G. L., Zhang, J., Shi, J. H., Liu, S. M., Li, F. M., et al. (2011). Distribution of dissolved aluminum in the Southern Yellow Sea: Influences of a dust storm and the spring bloom. *Marine Chemistry*, *125*(1–4), 69–81. https://doi.org/10.1016/j.marchem.2011.02.004

Romans, K. M., Carpenter, E. J., & Bergman, B. (1994). Buoyancy regulation in the colonial diazotrophic cyanobacterium *Trichodesmium tenue*: ultrastructure and storage of carbohydrate, polyphosphate, and nitrogen. *Journal of Phycology*, *30*(6), 935–942.

Rouco, M., Haley, S. T., & Dyhrman, S. T. (2016). Microbial diversity within the *Trichodesmium* holobiont. *Environmental Microbiology*, *18*(12), 5151–5160. https://doi.org/10.1111/1462-2920.13513

Rubin, M., Berman-Frank, I., & Shaked, Y. (2011). Dust- and mineral-iron utilization by the marine dinitrogen-fixer *Trichodesmium*. *Nature Geoscience*, *4*(8), 529–534. https://doi.org/10.1038/ngeo1181

Rueter, J. G., McCarthy, J. J., & Carpenter, E. J. (1979). The toxic effect of copper on Oscillatoria (*Trichodesmium*) *thiebautii*. *Limnology and Oceanography*, *24*(3), 558–562. https://doi.org/10.4319/lo.1979.24.3.0558

Schladitz, A., Müller, T., Kaaden, N., Massling, A., Kandler, K., Ebert, M., et al. (2009). *In situ* measurements of optical properties at Tinfou (Morocco) during the Saharan Mineral Dust Experiment SAMUM 2006. *Tellus, Series B: Chemical and Physical Meteorology*, *61*(1), 64–78. https://doi.org/10.1111/j.1600-0889.2008.00397.x

Shaked, Y., & Lis, H. (2012). Disassembling iron availability to phytoplankton. *Frontiers in Microbiology*, *3*(APR), 1–26. https://doi.org/10.3389/fmicb.2012.00123

Shaked, Y., de Beer, D., Wang, S., Zhang, F., Visser, A. N., Eichner, M., & Basu, S. (2023). Co-acquisition of mineral-bound iron and phosphorus by natural *Trichodesmium* colonies. *Limnology and Oceanography*, 1–14. https://doi.org/10.1002/lno.12329

Stockdale, A., Krom, M. D., Mortimer, R. J. G., Benning, L. G., Carslaw, K. S., Herbert, R. J., et al. (2016). Understanding the nature of atmospheric acid processing of mineral dusts in supplying bioavailable phosphorus to the oceans. *Proceedings of the National Academy of Sciences of the United States of America*, *113*(51), 14639–14644. https://doi.org/10.1073/pnas.1608136113

Tang, W., Cerdán-García, E., Berthelot, H., Polyviou, D., Wang, S., Baylay, A., et al. (2020). New insights into the distributions of nitrogen fixation and diazotrophs revealed by high-resolution sensing and sampling methods. *ISME Journal*, *14*(10), 2514–2526. https://doi.org/10.1038/s41396-020-0703-6

Villareal, T. A., & Carpenter, E. J. (2003). Buoyancy regulation and the potential for vertical migration in the oceanic cyanobacterium *Trichodesmium*. *Microbial Ecology*, *45*(1), 1–10. https://doi.org/10.1007/s00248-002-1012-5

Villareal, Tracy A., & Carpenter, E. J. (1990). Diel buoyancy regulation in the marine diazotrophic cyanobacterium *Trichodesmium thiebautii*. *Limnology and Oceanography*, *35*(8), 1832–1837. https://doi.org/10.4319/lo.1990.35.8.1832

Walsby, A. E. (1978). The properties and buoyancy-providing role of gas vacuoles in *Trichodesmium* Ehrenberg. *British Phycological Journal*, *13*(2), 103–116. https://doi.org/10.1080/00071617800650121

Walsby, A. E. (1992). The gas vesicles and buoyancy of *Trichodesmium*. In J. G. Carpenter, E.J., Capone, D.G., Rueter (Ed.), *Marine Pelagic Cyanobacteria: Trichodesmium and other Diazotrophs* (pp. 141–161). Springer, Dordrecht. https://doi.org/10.1007/978-94-015-7977-3_9

Wang, S., Koedooder, C., Zhang, F., Kessler, N., Eichner, M., Shi, D., & Shaked, Y. (2022). Colonies of the marine cyanobacterium *Trichodesmium* optimize dust utilization by selective collection and retention of nutrient-rich particles. *IScience*, *25*(1), 103587. https://doi.org/10.1016/j.isci.2021.103587

Wang, S., Zhang, F., Koedooder, C., Qafoku, O., Basu, S., Krisch, S., et al. (2023). Calculations and simulations of dust factor (K) and sinking velocity of particle-free *Trichodesmium* colonies (v0). *Zenodo*. https://doi.org/10.5281/zenodo.10290901

White, A. E., Spitz, Y. H., & Letelier, R. M. (2006). Modeling carbohydrate ballasting by *Trichodesmium* spp. *Marine Ecology Progress Series*, *323*(Oliver 1994), 35–45. https://doi.org/10.3354/meps323035

Yang, T., Chen, Y., Zhou, S., & Li, H. (2019). Impact of copper on marine phytoplankton: A Review. *Atmosphere*, *10*(414), 599–602. Retrieved from http://inis.iaea.org/search/search.aspx?orig_q=RN:41131251

Zehr, J. P., & Capone, D. G. (2020). Changing perspectives in marine nitrogen fixation. *Science*, *368*(6492). https://doi.org/10.1126/science.aay9514

Zhang, C., Ito, A., Shi, Z., Aita, M. N., Yao, X., Chu, Q., et al. (2019). Fertilization of the Northwest Pacific Ocean by East Asia Air Pollutants. *Global Biogeochemical Cycles*, *33*(6), 690–702. https://doi.org/10.1029/2018GB006146

Journal of Geophysical Research: Biogeosciences

Supplementary information for

Costs of dust collection by *Trichodesmium*: Effect on buoyancy and toxic metal release

Siyuan Wang [1,2], Futing Zhang [1,2], Coco Koedooder [1,2,3], Odeta Qafoku [4], Subhajit Basu [1,2,5], Stephan Krisch [8], Anna-Neva Visser [1,2], Meri Eichner [6], Nivi Kessler [1,2,9], Rene M. Boiteau [7], Martha Gledhill [8] and Yeala Shaked [1,2]

[1] The Freddy and Nadine Herrmann Institute of Earth Sciences, Edmond J. Safra Campus, Givat Ram, Hebrew University of Jerusalem, Jerusalem, Israel

[2] The Interuniversity Institute for Marine Sciences in Eilat, Eilat, Israel

[3] Israel Limnology and Oceanography Research, Haifa, Israel

[4] Environmental Molecular Sciences Laboratory (EMSL), Pacific Northwest National Laboratory (PNNL), Richland, WA, 99454, USA

[5] University of Petroleum and Energy Studies (UPES-SoHST), Energy Acres, Dehradun 248007, India

[6] Center Algatech, Institute of Microbiology of the Czech Academy of Sciences, Novohradská 237, 37981 Třeboň, Czech Republic

[7] Department of Chemistry, University of Minnesota, Minneapolis, MN 55455

[8] GEOMAR, Helmholtz Center for Ocean Research, Kiel, Germany

[9] Present address: The water authority, 7 Bank of Israel st, Jerusalem 9195021, Israel

Contents of this file:

Introduction:

This supplementary material provides readers with details regarding sedimentation experiments, toxicity assays and SEM-EDX analysis for examining the removal of toxic particles. **Sedimentation experiments** - experimental procedures (Fig. S1 and S2), raw data files (Table S1 and S2), modeling of colony sinking velocity (Text S1 and S2, Table S3, S4 and S5) and dust loss analysis (Text S3 and Fig. S3). **Toxicity assays** - experimental procedures (Text S4 and Fig. S4), colony mortality (incubated with $CuSO_4$; Fig. S5) and calculation of metal release (Table S6 and Fig. S6). Effective dust concentrations calculated for *in situ* colonies (Fig. S7) and colonies from incubations (Fig. S8). **SEM-EDX analysis** - experimental procedures (Fig. S9) and elemental maps (Fig. S10, S11, S12 and S13).

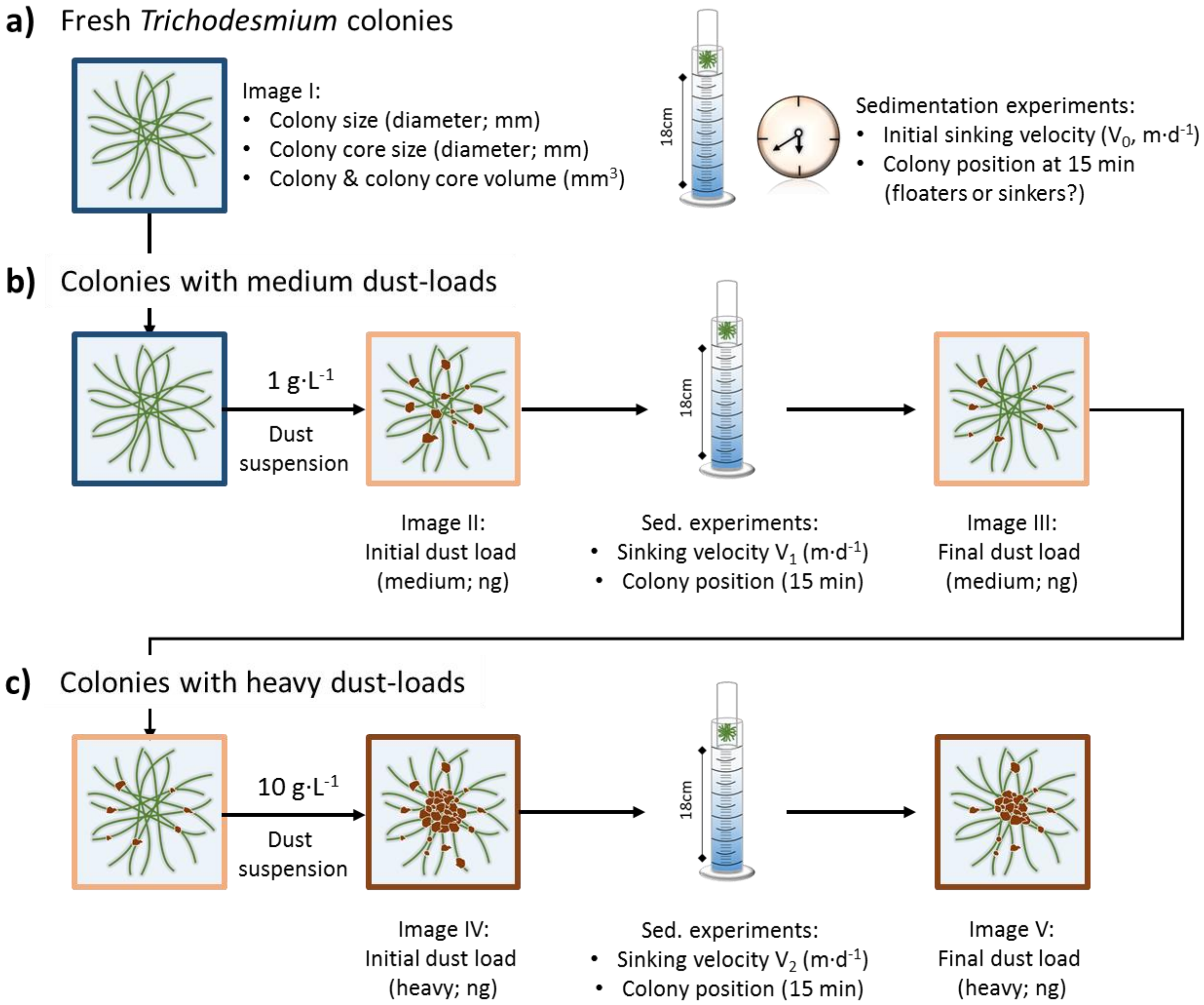

Figure S1. A schematic diagram of the experimental design for measuring the sinking velocity of a *Trichodesmium* colony at different dust loads.

The sinking velocity of *Trichodesmium* was measured on 5 individual days in the 2020 autumn season using 25 single colonies: without any dust particles (a) and with two manipulated dust-loads (medium and heavy, b and c).

(a) Freshly-collected colonies were first imaged under a stereoscope to determine their basic parameters (Image I). Each colony was then placed into a sedimentation chamber containing 100 mL fresh seawater using a 20 µL pipette equipped with cut tips to minimize the initial force added to the colony sinking velocity. Upon careful injection, a timer was started to measure the sinking time while the colony position (before reaching the bottom) was tracked and recorded by a researcher. The sinking velocity of a colony was calculated as the distance it travelled divided by time. Measurements of sinking velocity usually lasted less than 5 min, after which colonies were left in the same chamber and their positions at 15 min were observed. Some colonies remained at the bottom while others left the bottom and were relocated at different depth. We refer to these observations as indicators of the colony buoyancy and define those at the bottom as “sinkers” and the others as “floaters”.

(b) After measuring the initial sinking velocity (V_0), the colony was transferred with a long serological pipette into an eppendorf containing 1 $g \cdot L^{-1}$ dust suspension and mixed gently for loading dust particles (medium dust loads). Sinking velocity (V_1) measurements (and floatation status at 15 min) were performed using the same manner as described in (a). Stereoscopic images were taken prior to (Image II) and after experiments (Image III), for calculating initial and final dust loads via image analysis.

(c) Subsequently, the same colony was transferred into 10 $g \cdot L^{-1}$ dust suspension and mixed gently for measuring the sinking velocity (V_2) at heavy dust loads. Measurements of sinking velocity (V_2), determination of floatation status, as well as stereoscopic images (Image III and IV) were achieved in the same manner as described in (b).

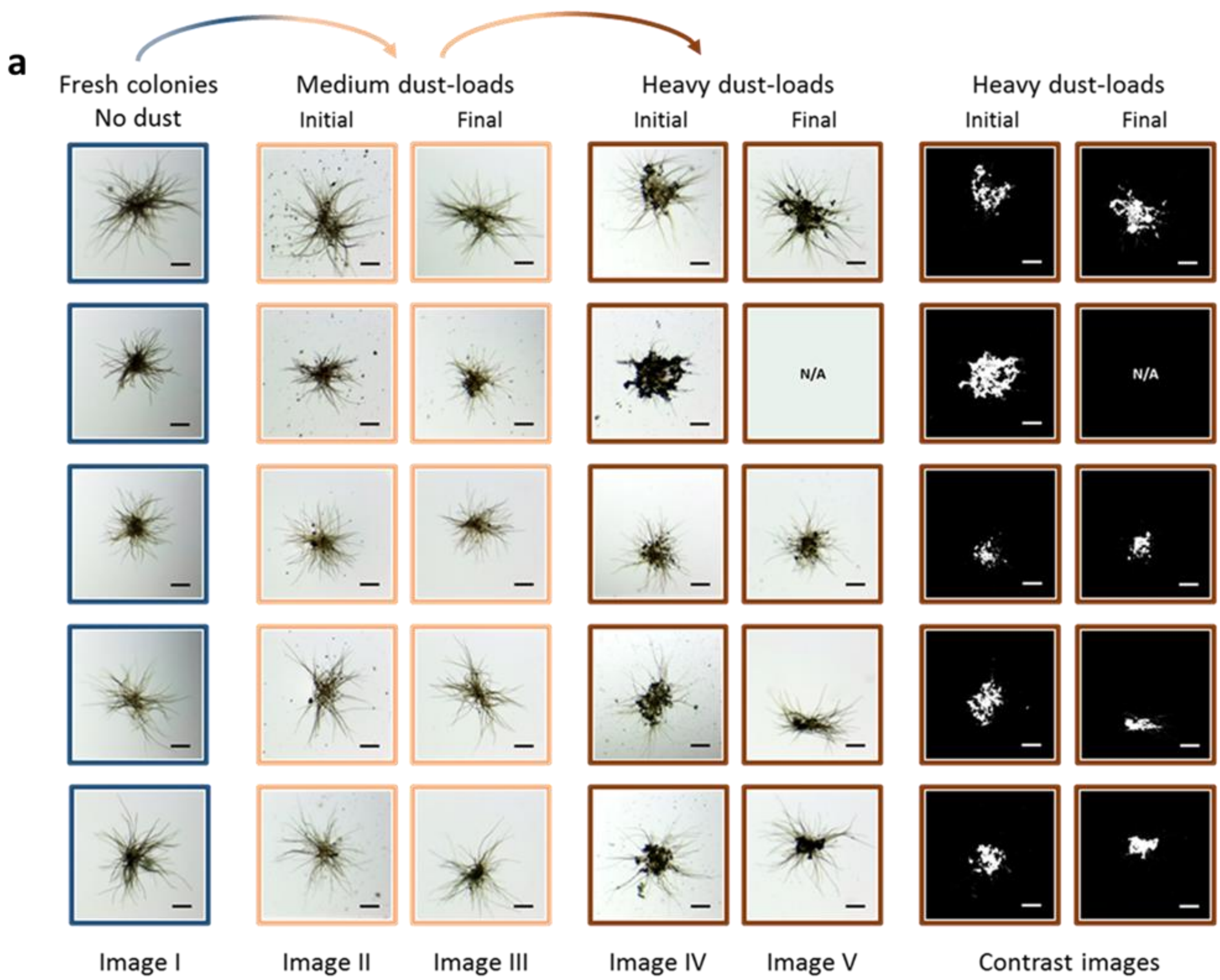

b

Sample	Image I (no dust)				Image II & III (medium)		Image IV & V (heavy)	
	Diameter (mm)		Volume (mm^3)		Dust loads (ng)			
	Colony	Colony core	Colony	Colony core	Initial	Final	Initial	Final
Colony 1	1.2	0.2	0.852	0.007	111	74	1400	1973
Colony 2	0.8	0.2	0.247	0.006	410	120	3475	N/A
Colony 3	0.8	0.2	0.232	0.006	214	109	597	697
Colony 4	1.0	0.3	0.592	0.009	140	49	1538	723
Colony 5	1.0	0.2	0.502	0.006	96	33	1224	1036

Figure S2. An example of image analysis – estimation of dust loads on five Red Sea colonies from sedimentation experiments conducted on October 18th, 2020.

(a) The size of colony and colony core was obtained from Image I using DinoCapture 2.0 software. To determine medium dust-loads (Image II and III), individual dust-covered area was measured using polygon tools and was summed to obtain the total dust-covered area (μm^2). To determine heavy dust-loads (Image IV and V), since dust particles were clustered in the colony core, total dust-covered area was obtained through pixel counting using contrast mode in ImageJ software. Total dust volume (μm^3) was subsequently derived by multiplying dust-covered area (μm^2) with an assumed constant thickness of 10 µm for the dust layer. Similar analysis was also conducted on natural dust loads of Red Sea (Eilat, this study) and Atlantic colonies (as reported by Held et al., 2022). All scale bars shown in the graph are 200 µm.

(b) A summary table of basic colony parameters and calculated medium and heavy dust loads for the colonies shown in panel a. The volume of colony and colony core was determined using the equation for calculating the sphere volume ($V=4/3 \cdot \pi \cdot r^3$). Dust loads were derived by multiplying total dust volume (μm^3) with a dust density of 2.5 $g \cdot cm^{-3}$. N/A means not available due to the colony loss during transfer.

Table S1. Image analysis of *in situ* dust loads for Red Sea and Atlantic *Trichodesmium* colonies; related to Fig. 1 in the main text.

Colony #	Collection date	Colony radius (mm)	Colony volume (µL)	Number of particles	Particle diameter (µm)	Total dust Volume (µm³)	Calculated dust weight[a] (ng)
1	10-Oct-18	0.644	1.1	1	N/A	7.4E+03	18
2	11-Oct-18	1.282	8.8	1	68	3.6E+04	91
3	15-Oct-18	0.814	2.3	7	10-26	3.9E+04	97
4	18-Oct-18	0.731	1.6	2	8-18	3.0E+03	8
5	18-Oct-18	0.464	0.4	4	18-20	1.1E+04	29
6	18-Oct-18	0.501	0.5	4	16-30	1.7E+04	42
7	28-Oct-18	0.760	1.8	3	12	5.9E+04	148
8	29-Oct-18	0.587	0.8	2	18-22	6.3E+03	16
9	29-Oct-18	0.477	0.5	1	40	1.3E+04	31
10	31-Oct-18	0.927	3.3	5	30-38	6.7E+04	167
11	1-Nov-18	0.689	1.4	1	16	2.0E+03	5
12	1-Nov-18	0.606	0.9	2	30-48	2.5E+04	63
13	1-Nov-18	0.557	0.7	2	16	4.4E+04	111
14	1-Nov-18	0.479	0.5	1	N/A	3.3E+03	8
15	6-Nov-18	0.469	0.4	2	10-16	2.8E+03	7
16	6-Nov-18	0.442	0.4	1	30	7.1E+03	18
17	7-Nov-18	0.560	0.7	2	20	9.4E+03	23
18	15-Nov-18	0.602	0.9	1	16	2.0E+03	5
19	7-May-19	0.887	2.9	2	12-18	3.7E+03	9
20	15-May-19	0.937	3.4	1	48	1.8E+04	45
21	15-May-19	0.572	0.8	1	18	2.5E+03	6
22	22-May-19	0.454	0.4	1	12	1.1E+03	3
23	22-May-19	0.658	1.2	1	N/A	2.1E+04	53
24	22-May-19	0.479	0.5	2	12-26	6.4E+03	16
Min.		0.442	0.4	1	8	1.1E+03	3
Max.		1.282	8.8	7	68	6.7E+04	167
Median.		0.595	0.9	2	18	8.4E+03	21
Held et al. (2021)	Fig. 1c	0.776	2.0	-	-	5.4E+06	13461
	Fig. 1d	0.763	1.9	-	-	6.0E+06	14999
	Fig. 1e	0.792	2.1	-	-	4.0E+06	9954
	Fig. 1f	0.776	2.0	-	-	1.8E+06	4486

a. Dust weight (ng) was derived by multiplying the volume of dust particles (μm^3) with a dust density of 2.5 $g \cdot cm^{-3}$.
b. N/A means not available because the particle diameter was too small to be measured.

Table S2. Data pairs of colony dust load and sinking velocity during sedimentation experiments (n=75). The data for six representative colonies (colored red) analyzed on October 18th and October 20th 2020 was plotted in Fig. 2 in the main text.

Data pairs	Exp. date	Colony ID	Colony radius	Treatments	Dust weight (ng)		Sinking velocity	Floatation status at 15 min
			mm		Initial	Final	$m \cdot d^{-1}$	
1	18-Oct-20	A	0.588	No dust	-	-	64	Floater
2				Medium	111	74	119	Sinker
3				Heavy	1400	1973	141	Sinker
4		B	0.389	No dust	-	-	64	Sinker
5				Medium	410	120	53	Floater
6				Heavy	3475	Colony lost	351	Sinker
7		C	0.381	No dust	-	-	38	Floater
8				Medium	214	109	47	Sinker
9				Heavy	597	697	75	Sinker
10		D	0.521	No dust	-	-	58	Floater
11				Medium	140	49	34	Sinker
12				Heavy	1538	723	38	Sinker
13		E	0.493	No dust	-	-	45	Floater
14				Medium	96	33	45	Sinker
15				Heavy	1224	1036	131	Sinker
16	20-Oct-20	F	0.502	No dust	-	-	22	Floater
17				Medium	649	512	198	Sinker
18				Heavy	4065	2752	479	Sinker
19		G	0.504	No dust	-	-	26	Floater
20				Medium	168	51	41	Floater
21				Heavy	4419	2221	211	Sinker
22		H	0.454	No dust	-	-	32	Floater
23				Medium	114	38	66	Sinker
24				Heavy	3045	133	83	Sinker
25		I	0.433	No dust	-	-	37	Floater
26				Medium	1405	648	114	Sinker
27				Heavy	2721	1345	161	Sinker
28		J	0.532	No dust	-	-	21	Floater
29				Medium	1053	559	142	Sinker
30				Heavy	1910	2747	277	Sinker
31	21-Oct-20	K	0.376	No dust	-	-	42	Floater
32				Medium	16	20	144	Floater
33				Heavy	2442	39	220	Sinker
34		L	0.410	No dust	-	-	33	Floater
35				Medium	69	2	234	Sinker
36				Heavy	2997	40	251	Sinker

37		M	0.499	No dust	-	-	50	Sinker
38				Medium	166	43	158	Sinker
39				Heavy	2621	56	180	Sinker
40		N	0.482	No dust	-	-	38	Floater
41				Medium	132	101	221	Floater
42				Heavy	4024	3128	351	Sinker
43		O	0.566	No dust	-	-	50	Floater
44				Medium	68	58	243	Sinker
45				Heavy	1872	1290	129	Sinker
46	22-Oct-20	P	0.399	No dust	-	-	37	Floater
47				Medium	53	7	216	Floater
48				Heavy	951	31	102	Sinker
49		Q	0.420	No dust	-	-	20	Floater
50				Medium	85	37	237	Floater
51				Heavy	2343	759	144	Sinker
52		R	0.393	No dust	-	-	36	Floater
53				Medium	38	74	65	Floater
54				Heavy	1021	1403	65	Sinker
55		S	0.373	No dust	-	-	25	Floater
56				Medium	50	5	198	Sinker
57				Heavy	497	61	65	Sinker
58		T	0.435	No dust	-	-	14	Floater
59				Medium	99	62	144	Sinker
60				Heavy	2561	1628	186	Sinker
61	26-Oct-20	U	0.543	No dust	-	-	53	Sinker
62				Medium	114	48	211	Sinker
63				Heavy	1089	84	16	Floater
64		V	0.445	No dust	-	-	37	Floater
65				Medium	82	18	138	Sinker
66				Heavy	2075	1155	23	Sinker
67		W	0.457	No dust	-	-	0	Floater
68				Medium	61	9	122	Floater
69				Heavy	334	174	52	Floater
70		X	0.399	No dust	-	-	36	Floater
71				Medium	55	5	113	Floater
72				Heavy	1508	765	59	Sinker
73		Y	0.689	No dust	-	-	11	Floater
74				Medium	153	210	156	Sinker
75				Heavy	409	675	23	Floater

Supplementary text S1. Modeling the sinking velocity of natural *Trichodesmium* colonies loaded with dust particles.

The sinking velocity of a *Trichodesmium* colony can be calculated according to Stoke's Law (Kromkamp & Walsby, 1990; White et al., 2006), using the following equation:

$$v = \frac{2gr^2(\rho_c - \rho_w)A}{9\phi\eta} \quad (eq. 1)$$

Where: ***v*** **–** colony sinking velocity ($m \cdot s^{-1}$); ***g*** **–** gravitational acceleration ($m \cdot s^{-2}$); ***r*** **–** colony radius (m); $\boldsymbol{\rho_C}$ and $\boldsymbol{\rho_W}$ **–** colony and seawater density, respectively ($kg \cdot m^{-3}$); ***A*** **–** cell volume to colony volume ratio; ***Φ*** **–** coefficient of form resistance; ***η*** **–** molecular viscosity of the medium ($kg \cdot m^{-1} \cdot s^{-1}$). ***A*** is the ratio of cell volume to colony volume, since most of space within colony sphere is occupied by seawater. For instance, ***A*** was assigned a value of 0.05 in the study by White et al. (2006), indicating that the colony sphere consists of 5% cell volume and 95% seawater volume.

We considered the significant change of $\boldsymbol{\rho_C}$ and ***A*** for *Trichodesmium* colonies after interacting with dust particles. Assuming that dust volume did not exceed the colony volume, new $\boldsymbol{\rho_C}$ and ***A*** can be derived as follows:

$$\rho' = \rho_{colony+dust} = \frac{m_{cell} + m_{dust}}{V_{cell} + V_{dust}} \quad (eq. 2)$$

$$A' = \frac{V_{cell} + V_{dust}}{V_{colony}} \quad (eq. 3)$$

$$V_{colony} = \frac{4}{3}\pi r^3 \quad (eq. 4)$$

Where in eq.2: ***ρ'*** **–** the new density of a colony with dust ($kg \cdot m^{-3}$); $\boldsymbol{m_{cell}}$ and $\boldsymbol{m_{dust}}$ **–** cell and dust mass, respectively (kg); $\boldsymbol{V_{cell}}$ and $\boldsymbol{V_{dust}}$ **–** cell and dust volume, respectively (m^3). Where in eq.3: ***A'*** **–** cell and dust volume to colony volume ratio; $\boldsymbol{V_{cell}}$, $\boldsymbol{V_{dust}}$ and $\boldsymbol{V_{colony}}$ are cell, dust and colony volume, respectively (m^3). Where in eq.4: $\boldsymbol{V_{colony}}$ **–** colony volume (m^3); ***r*** **–** colony radius (m). Substituting equation 2, 3 and 4 into equation 1 and performing integration, the sinking velocity of a colony with dust particles (***v'***) is derived as follows:

$$v' = v_{colony+dust} = \frac{g}{6\pi r\phi\eta}[m_{dust} - \rho_w V_{dust} + m_{cell} - \rho_w V_{cell}] \quad (eq. 5)$$

Since:

$$V_{dust} = \frac{m_{dust}}{\rho_{dust}} \quad (eq. 6); \quad V_{cell} = \frac{m_{cell}}{\rho_{cell}} \quad (eq. 7)$$

Where: $\boldsymbol{\rho_{dust}}$ and $\boldsymbol{\rho_{cell}}$ **–** *Trichodesmium* dust density and cell density, respectively ($kg \cdot m^{-3}$). Substituting equation 6 and 7 into equation 5 derives equation 8:

$$v' = m_{dust} \cdot \frac{g\left(1 - \frac{\rho_w}{\rho_{dust}}\right)}{6\pi r\phi\eta} + m_{cell} \cdot \frac{g\left(1 - \frac{\rho_w}{\rho_{cell}}\right)}{6\pi r\phi\eta} \quad (eq.8)$$

Where: ***v'* –** the sinking velocity of colony with dust particles (m·s^{-1}); $\boldsymbol{m_{dust}}$ and $\boldsymbol{m_{cell}}$ **–** dust and cell mass, respectively (kg); ***g* –** gravitational acceleration (m·s^{-2}); $\boldsymbol{\rho_W}$, $\boldsymbol{\rho_{dust}}$ and $\boldsymbol{\rho_{cell}}$ **–** seawater, dust and cell density, respectively (kg·m^{-3}); ***r* –** colony radius (m); ***Φ* –** coefficient of form resistance; ***η* –** molecular viscosity of the medium (kg·m^{-1}·s^{-1}).

$$K = \frac{g\left(1 - \frac{\rho_w}{\rho_{dust}}\right)}{6\pi r\phi\eta} \quad (eq.9); \quad v_0 = m_{cell} \cdot \frac{g\left(1 - \frac{\rho_w}{\rho_{cell}}\right)}{6\pi r\phi\eta} \quad (eq.10)$$

Equation 8 predicts a linear increase of velocity (***v'***) with increasing dust weight ($\boldsymbol{m_{dust}}$). The slope (dust factor-K) is influenced by colony size (***r***), seawater ($\boldsymbol{\rho_W}$) and dust density ($\boldsymbol{\rho_{dust}}$). The intercept (sinking velocity when the colony is particle-free; herein defined as "***v0***") is influenced by cell mass ($\boldsymbol{m_{cell}}$), colony size (***r***), seawater ($\boldsymbol{\rho_W}$) and cell density ($\boldsymbol{\rho_{cell}}$). When dust load is zero, the intercept (***v0***) can be converted to equation 1 using equation 3. Calculations and simulations of dust factor (K) and sinking velocity of particle-free colonies (***v0***) are described in supplementary text S2.

Supplementary text S2. Calculations and simulations of dust factor (K) and sinking velocity of particle-free colonies (*v0*).

Using python (Version 3.10.9) with a *linspace* function, we first simulated the range of dust factors (K) derived from equation 8, using parameter values obtained from this study and literatures (see Table S3). During the simulation, seawater and dust density and colony radius (***ρ_{water}, ρ_{dust}*** and ***r***) were set to be variants, while the remaining parameters were fixed to literature values. The simulated dust factor (K) ranged from 2.2-7.4 x 10^5 m·s^{-1}·kg^{-1} (0.02-0.06 m·d^{-1}·ng^{-1}). All python codes related to the calculation of dust factor (K) can be found in Github (*https://github.com/Zhanzhu1110/Trichobuoyancy.git*), as well as in Zenodo (*https://zenodo.org/records/10290901*; DOI:10.5281/zenodo.10290901)(Wang et al., 2023).

Table S3. The equation and parameter values for calculating dust factor (K)

Dust factor (K)	Para-meters	Definitions	Parameter range	Units	Source
$\frac{g\left(1-\frac{\rho_w}{\rho_{dust}}\right)}{6\pi r\phi\eta}$	K	Dust factor	2.2 x 10^5 to 7.4 x 10^5	m·s^{-1}·kg^{-1}	Simulation results
	ρ_w	Seawater density	Variable[a]	kg·m^{-3}	Benaltabet et al. (2022)
	ρ_{dust}	Dust density	Variable[b]	kg·m^{-3}	McConnell et al. (2008); Schladitz et al. (2009)
	r	Colony radius	Variable[c]	m	This study (Table S2)
	g	Gravitational acceleration	9.81	m·s^{-2}	Wikipedia[d]
	Φ	Form resistance	1	-	White et al. (2006)
	η	Dynamic viscosity	9.60 x 10^{-4}	kg·m^{-1}·s^{-1}	White et al. (2006)

a. The range of seawater densities (ρ_W) is from 1026.5 to 1029 kg·m^{-3} (Rea Sea surface to ca. 700m).

b. The range of dust densities (ρ_{dust}) is from 2100 to 2600 kg·m^{-3}.

c. The range of colony radius (r) is from 0.442 to 1.282 mm (measured on Red Sea colonies, see Table S2).

d. *https://en.wikipedia.org/wiki/Gravity_of_Earth*

Simulation of sinking velocity of particle-free colonies (***v0***) requires the key parameter of cell mass (***m_{cell}***) or more specifically, the cell volume (***V_{cell}***; see Table S4 for ***V_{cell}*** estimation). Using equation 7 and 10, the equation for calculating ***v0*** is derived as follows:

$$v_0 = \frac{g \cdot V_{cell} \cdot (\rho_{cell} - \rho_W)}{6\pi r\phi\eta} \quad (eq. 11)$$

Where: ***v0*** **–**the sinking velocity of particle-free colonies (m·s^{-1}); ***V_{cell}*** **–** cell volume (m^3); ***ρ_{cell}*** and ***ρ_W*** **–** cell and seawater density, respectively (kg·m^{-3}); ***r*** **–** colony radius (m); ***Φ*** **–** coefficient of form resistance; ***η*** **–** molecular viscosity of the medium (kg·m^{-1}·s^{-1}). During the simulation, four parameters (***V_{cell}, ρ_{cell}, ρ_{water}*** and

r) were set to be variants, while the rest parameters were fixed to literature values (see Table S5). Using python, we obtained the sinking velocity of particle-free colonies ranged between 9.9 x 10^{-7}- 1.1 x 10^{-4} m·s^{-1} (0 to 9 m·d^{-1}). All python codes related to the calculation of ***v0*** can be found in Github (*https://github.com/Zhanzhu1110/Trichobuoyancy.git*) and Zenodo (*https://zenodo.org/records/10290901*; DOI:10.5281/zenodo.10290901)(Wang et al., 2023).

Table S4. Estimation of total cell volume (*V_{cell}*) in single Red Sea *Trichodesmium* colonies

Trichodesmium	Single cell volume	Cell number	Total cell volume[a]	Source
	µm^3	#	µm^3	
Tuft colonies	-	-	3.9 x 10^5	Benavides et al. (2022) - SI
Puff colonies (Eilat)	83-209[b]	4708-11088	3.9 -23 x 10^5	Basu and Shaked (2018) - Table SI-B

a. Total cell volume (µm^3) was derived by multiplying the single cell volume (µm^3) with cell number (#).

b. Single cell volume (µm^3) was derived by considering the cell as a cylinder (V=πr^2*d). Cell radius (r) and cell length (d) used here ranged between 2.4-2.9 µm and 4.8-8.2 µm, respectively (Basu & Shaked, 2018). Calculated single cell volume is similar to the results of *Trichodesmium* IMS101 culture, as reported by Ho (2013).

Table S5. Equation and parameter values for calculating sinking velocity of particle-free colonies (*v0*)

v0	Para-meters	Definitions	Parameter range	Units	Source
$\frac{g \cdot V_{cell} \cdot (\rho_{cell} - \rho_w)}{6\pi r \phi \eta}$	*v0*	Sinking velocity (particle-free)	9.9 x 10^{-7} to 1.1 x 10^{-4}	m·s^{-1}	Simulation results
	V_{cell}	Cell volume	Variable[a]	m^3	Table S4
	ρ_{cell}	Cell density	Variable[b]	kg·m^{-3}	White et al. (2006)
	ρ_w	Seawater density	Variable[c]	kg·m^{-3}	Benaltabet et al. (2022)
	r	Colony radius	Variable[d]	m	This study (Table S2)
	g	Gravitational acceleration	9.81	m·s^{-2}	Wikipedia[e]
	Φ	Form resistance	1	-	White et al. (2006)
	η	Dynamic viscosity	9.60 x 10^{-4}	kg·m^{-1}·s^{-1}	White et al. (2006)

a. The range of cell volume is from 3.9 -23 x 10^5 µm^3 (see Table S4)

b. The range of a sinking cell density (ρ_{cell}) is from 1035 to 1065 kg·m^{-3}, as reported by White et al. (2006).

c. The range of seawater density (ρ_w) is from 1026.5 to 1029 kg·m^{-3} (sea surface to ca. 700m).

d. The range of colony radius (r) is from 0.442 to 1.282 mm (measured on Red Sea colonies, see Table S2).

e. *https://en.wikipedia.org/wiki/Gravity_of_Earth*

Table S6. Calculation of dust loss on *Trichodesmium* colonies during sedimentation experiments.

Data pairs	Exp. date	Colony ID	Colony radius	Colony volume		Dust load		Dust loss
						ng		
			mm	mm^3; µL	Treatments	Initial	Final	ng
1	18-Oct-20	A	0.588	0.852	Medium	111	74	37
2					Heavy	1400	1973	No loss
3		B	0.389	0.247	Medium	410	120	290
4					Heavy	3475	Colony lost	Colony lost
5		C	0.381	0.232	Medium	214	109	105
6					Heavy	597	697	No loss
7		D	0.521	0.592	Medium	140	49	90
8					Heavy	1538	723	815
9		E	0.493	0.502	Medium	96	33	63
10					Heavy	1224	1036	188
11	20-Oct-20	F	0.502	0.530	Medium	649	512	137
12					Heavy	4065	2752	1313
13		G	0.504	0.536	Medium	168	51	117
14					Heavy	4419	2221	2198
15		H	0.454	0.392	Medium	114	38	75
16					Heavy	3045	133	2912
17		I	0.433	0.340	Medium	1405	648	757
18					Heavy	2721	1345	1376
19		J	0.532	0.631	Medium	1053	559	494
20					Heavy	1910	2747	No loss
21	21-Oct-20	K	0.376	0.223	Medium	16	20	No loss
22					Heavy	2442	39	2403
23		L	0.410	0.289	Medium	69	2	67
24					Heavy	2997	40	2957
25		M	0.499	0.520	Medium	166	43	123
26					Heavy	2621	56	2564
27		N	0.482	0.469	Medium	132	101	31
28					Heavy	4024	3128	896
29		O	0.566	0.760	Medium	68	58	10
30					Heavy	1872	1290	582

31	22-Oct-20	P	0.399	0.266	Medium	53	7	46
32					Heavy	951	31	920
33		Q	0.420	0.310	Medium	85	37	48
34					Heavy	2343	759	1584
35		R	0.393	0.254	Medium	38	74	No loss
36					Heavy	1021	1403	No loss
37		S	0.373	0.217	Medium	50	5	45
38					Heavy	497	61	435
39		T	0.435	0.345	Medium	99	62	36
40					Heavy	2561	1628	932
41	26-Oct-20	U	0.543	0.671	Medium	114	48	65
42					Heavy	1089	84	1005
43		V	0.445	0.369	Medium	82	18	64
44					Heavy	2075	1155	920
45		W	0.457	0.400	Medium	61	9	52
46					Heavy	334	174	161
47		X	0.399	0.266	Medium	55	5	50
48					Heavy	1508	765	744
49		Y	0.689	1.370	Medium	153	210	No loss
50					Heavy	409	675	No loss

Treatments	Dust loss (ng)	
Medium	Min	10
	Max	757
Heavy	Min	161
	Max	2957

Supplementary text S3. Selection criterion for data pairs presented in Fig. 3, related to the main text - Section 3.1.3.

To illustrate the effect of dust loss on colony sinking velocity, we selected 20 out of 50 total data pairs obtained from sedimentation experiments and showed seven representative data pairs in Fig. 3 and the rest in Fig. S3 (n=13). The selected data pairs/colonies meet the following requirements: 1) calculation of dust loss was found to be positive values (42 out of 50 total data pairs) and 2) measured sinking velocities of these colonies against their initial dust loads plotted below the prediction line established in Fig. 2b ($y = 0.06\ m \cdot d^{-1} \cdot ng^{-1}$ x dust weight (ng) + $53\ m \cdot d^{-1}$; 20 out of 42 data pairs).

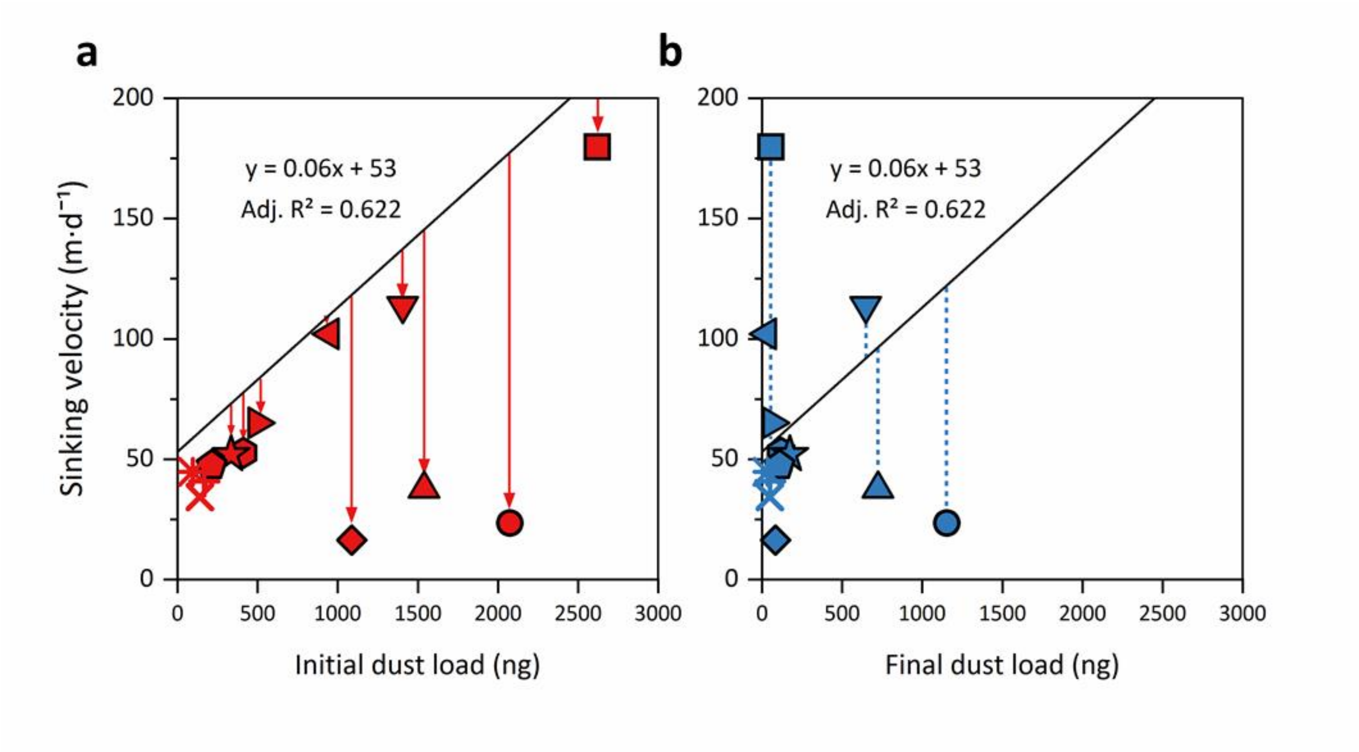

Figure S3. Effect of dust loss on colony sinking velocity. Measured sinking velocities of additional colonies (n=13, shown as different symbols) plotted against their initial (a) and final (b) dust loads, related to the main text – Fig.3. The equation (black line) is the linear relationship established in the main text - Fig. 2b. Arrows and dash lines indicate the mismatch of measured sinking velocities and expected velocities calculated from initial and final dust loads, respectively.

Supplementary text S4. Toxicity assays – incubation experiments on Red Sea *Trichodesmium* colonies with dust suspension, dust leachates and dissolved Cu ($CuSO_4$) and visual examinations of colony mortality during incubations.

To investigate the particle toxicity to *Trichodesmium*, we conducted incubations experiments on colonies with dust suspension and leachate for 24 hrs during the spring of 2022 (n=176; see main text – section 2.3). Simultaneously, similar incubation assays were conducted on Red Sea colonies with dissolved Cu ($CuSO_4$).

Primary $CuSO_4$ solutions were prepared daily in Milli-Q water (18.2 Ω) and diluted to final concentrations of 5, 10, 50, 200, 250, 500, 1000, and 3000 nM using filtered seawater (FSW). Two colonies per well were incubated in a 48-well plate containing 0.5 mL $CuSO_4$ solutions and were kept in a culture room (25 ^oC, ~80 $\mu E\ m^{-2} \cdot s^{-1}$, 10:14 h light-dark cycle) for up to 74 hrs. Visual examination of colony and filament shape, structure, and color was performed under a stereoscope (Fig. S4). Incubation of colonies without $CuSO_4$ addition served as control. Incubations with dissolved Cu were repeated thrice using freshly-collected Red Sea colonies (n=118).

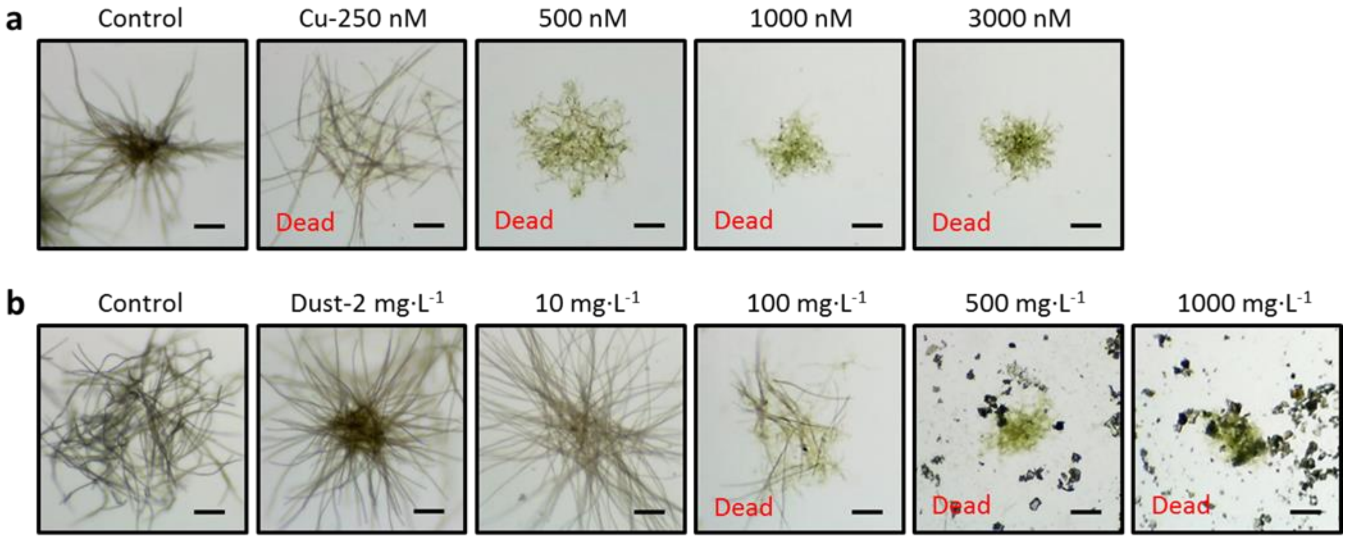

Figure S4. Stereoscopic observations of Red Sea *Trichodesmium* colonies when exposed to $CuSO_4$ (a) and dust suspensions (b) for 24 hrs. All scale bars are 200 μm. The mortality of *Trichodesmium* (%) was calculated by diving the number of dead colonies to the total number of colonies used in each treatment. Colonies identified as "dead" colonies were marked accordingly in the images.

Addition of 3000 nM $CuSO_4$ induced an acute toxicity to *Trichodesmium*, with 100% of colonies dead in 2hrs. Moreover, no colonies survived when incubating with >200 nM $CuSO_4$ for 24 hrs. Incubating with 5-50 nM Cu for 24 hrs yields 30-50% mortality of colonies (Fig. S5).

Applying Chlorophyll *a* (Chl *a*) content measured on Red Sea colonies (~5 ng Chl *a* colony^{-1}; unpublished data), we determined the lethal dose 100 (LD100) of Cu as 0.6 μg total Cu · (μg Chl *a*)$^{-1}$ (when total [Cu] = 200 nM). It is important to note that we reported the toxicity threshold of Cu with a unit of total Cu per biomass in this study, yet the toxicity does not depend on the total Cu added but rather on free (non-complexed) Cu concentrations (Paytan et al., 2009; Sunda & Huntsman, 1998). The toxicity threshold of Cu for

Trichodesmium was comparable to the Cu threshold for *Synechococcus* WH8102 (0.2 - 2 µg Cu · (µg Chl *a*)$^{-1}$), as reported by Paytan et al. (2009).

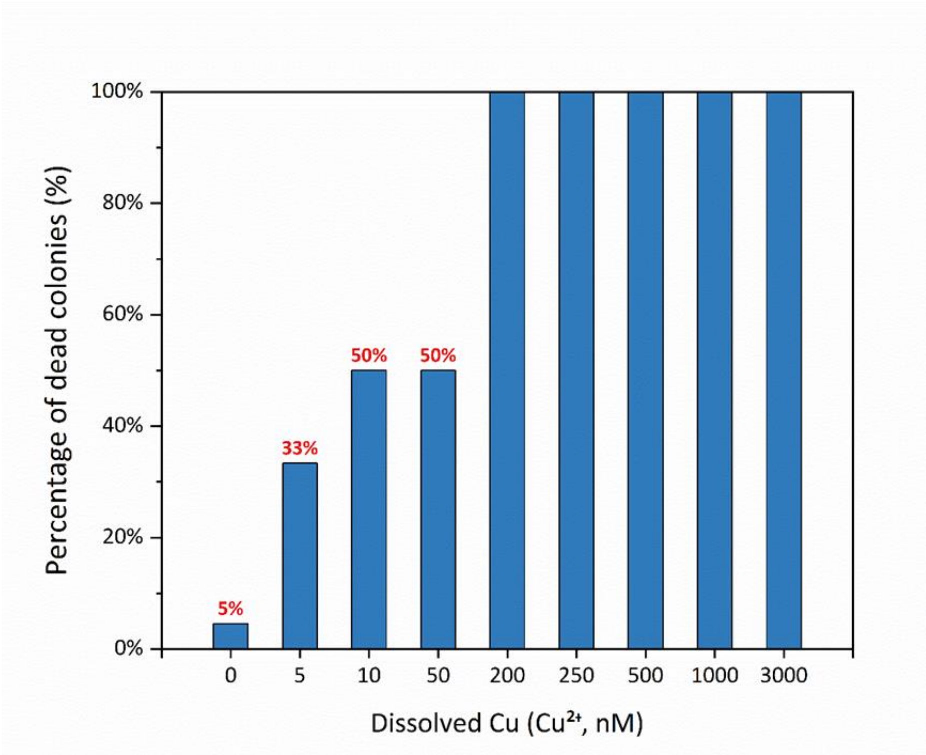

Figure S5. Percentage (%) death of Red Sea colonies after a 24-hour incubation with varying concentrations of dissolved Cu ($CuSO_4$) in seawater. The mortality was determined by dividing the number of dead colonies by the total colonies in each treatment prior to the incubation.

Table S7. Compilation data of seawater soluble aerosol metal in nM (aerosol concentrations = 2-42 mg·L^{-1}; data were obtained from this study and from Mackey et al., 2015 – Supplemental Table 2). Values were corrected using the average values of two operational blanks (seawater). Dissolution data were separated into rapid (<6 hrs) and gradual (1-7 days) dissolution and their median values were calculated. Boxes colored in green and red indicate dissolution of the same dust particles, respectively.

Data source		This study		Mackey et al. (2015)						
[Dust] mg·L^{-1}		2	10	17	22	22	27	30	33	42
Metal	Dissolution time	[Metal] nM								
Ni	10min			0.1	4.3	0.7	2.5	4.2	1.1	5.5
	6h			2.6	6.4	2.1	2.9	6.1	3.3	8.4
	Rapid (Median)	1.5	0.6	1.4	5.4	1.4	2.7	5.1	2.2	6.9
	1d			1.3	5.3	1.1	3.4	5.1	2.2	7.6
	3d			1.7	6.1	1.7	4.1	6.0	2.7	8.3
	7d			2.5	7.4	2.3	4.7	6.6	3.8	9.1
	Gradual (Median)	0.3	0.0	1.7	6.1	1.7	4.1	6.0	2.7	8.3
Zn	10min			42	82	27	59	201	54	99
	6h			55	96	38	65	226	55	107
	Rapid	0	33	49	89	32	62	214	54	103
	1d			52	97	35	69	226	54	105
	3d			50	97	36	71	221	54	106
	7d			52	109	35	68	202	61	111
	Gradual	0	40	52	97	35	69	221	54	106
Pb	10min			3.4	2.9	6.8	3.4	5.2	9.4	6.2
	6h			3.7	2.8	7.9	3.2	3.8	9.3	7.3
	Rapid	1.5		3.6	2.9	7.3	3.3	4.5	9.3	6.7
	1d			3.1	2.4	7.3	2.7	2.9	7.9	6.2
	3d			3.1	2.2	7.0	2.7	2.5	7.3	6.0
	7d			2.9	2.0	6.8	2.4	2.2	7.1	5.9
	Gradual	2.2		3.1	2.2	7.0	2.7	2.5	7.3	6.0
Co	10min			0.4	0.7	0.4	0.7	0.8	0.5	0.6
	6h			0.3	0.7	0.9	0.5	1.7	1.2	0.6
	Rapid	0.2	0.3	0.4	0.7	0.7	0.6	1.3	0.9	0.6
	1d			0.0	0.3	0.0	0.2	1.1	0.3	0.4
	3d			0.3	0.7	0.5	0.7	0.8	0.7	0.7
	7d			0.4	0.6	0.5	0.7	1.0	0.7	0.7
	Gradual	0.0	0.3	0.3	0.6	0.5	0.7	1.0	0.7	0.7
Cu	10min			3.1	8.4	0.8	5.8	4.8	1.3	5.8
	6h			5.6	11.8	1.5	7.9	8.1	2.1	8.7
	Rapid	0.4	1.8	4.3	10.1	1.2	6.8	6.4	1.7	7.3
	1d			6.3	13.1	1.8	8.9	9.2	2.7	9.5
	3d			5.7	12.1	1.6	9.0	9.0	2.7	8.8
	7d			5.6	11.9	1.3	9.3	8.2	2.3	8.8
	Gradual	1.0	1.1	5.7	12.1	1.6	9.0	9.0	2.7	8.8

Cd	10min			0.4	0.5	0.1	0.5	0.5	0.1	0.3
	6h			0.4	0.4	0.0	0.4	0.5	0.1	0.3
	Rapid	0.0	0.1	0.4	0.4	0.1	0.5	0.5	0.1	0.3
	1d			0.4	0.4	0.0	0.4	0.5	0.0	0.3
	3d			0.4	0.4	0.0	0.4	0.5	0.1	0.3
	7d			0.4	0.5	0.0	0.4	0.5	0.1	0.3
	Gradual	0.1	0.3	0.4	0.4	0.0	0.4	0.5	0.1	0.3
Mn	10min			35	72	28	62	108	46	46
	6h			41	86	39	70	137	64	52
	Rapid	1	17	38	79	33	66	122	55	49
	1d			41	89	42	74	140	68	54
	3d			41	92	43	76	147	70	55
	7d			43	96	47	75	148	75	56
	Gradual	0	15	41	92	43	75	147	70	55
Al	10min			35	38	17	30	60	21	115
	6h			67	83	56	82	171	75	176
	Rapid			51	61	37	56	116	48	146
	1d			82	105	80	112	236	151	193
	3d			114	129	190	144	327	253	211
	7d			135	180	310	180	441	421	198
	Gradual			114	129	190	144	327	253	198
Fe	10min			3.2	4.7	1.0	5.3	10.6	0.0	8.2
	6h			0.8	2.3	0.0	1.1	8.4	0.0	16.7
	Rapid			2.0	3.5	0.5	3.2	9.5	0.0	12.5
	1d			0.4	0.9	0.0	0.6	4.2	0.0	8.1
	3d			0.0	4.7	0.0	0.0	5.9	0.0	4.4
	7d			0.0	0.0	0.0	4.1	4.4	6.1	0.0
	Gradual			0.0	0.9	0.0	0.6	4.4	0.0	4.4

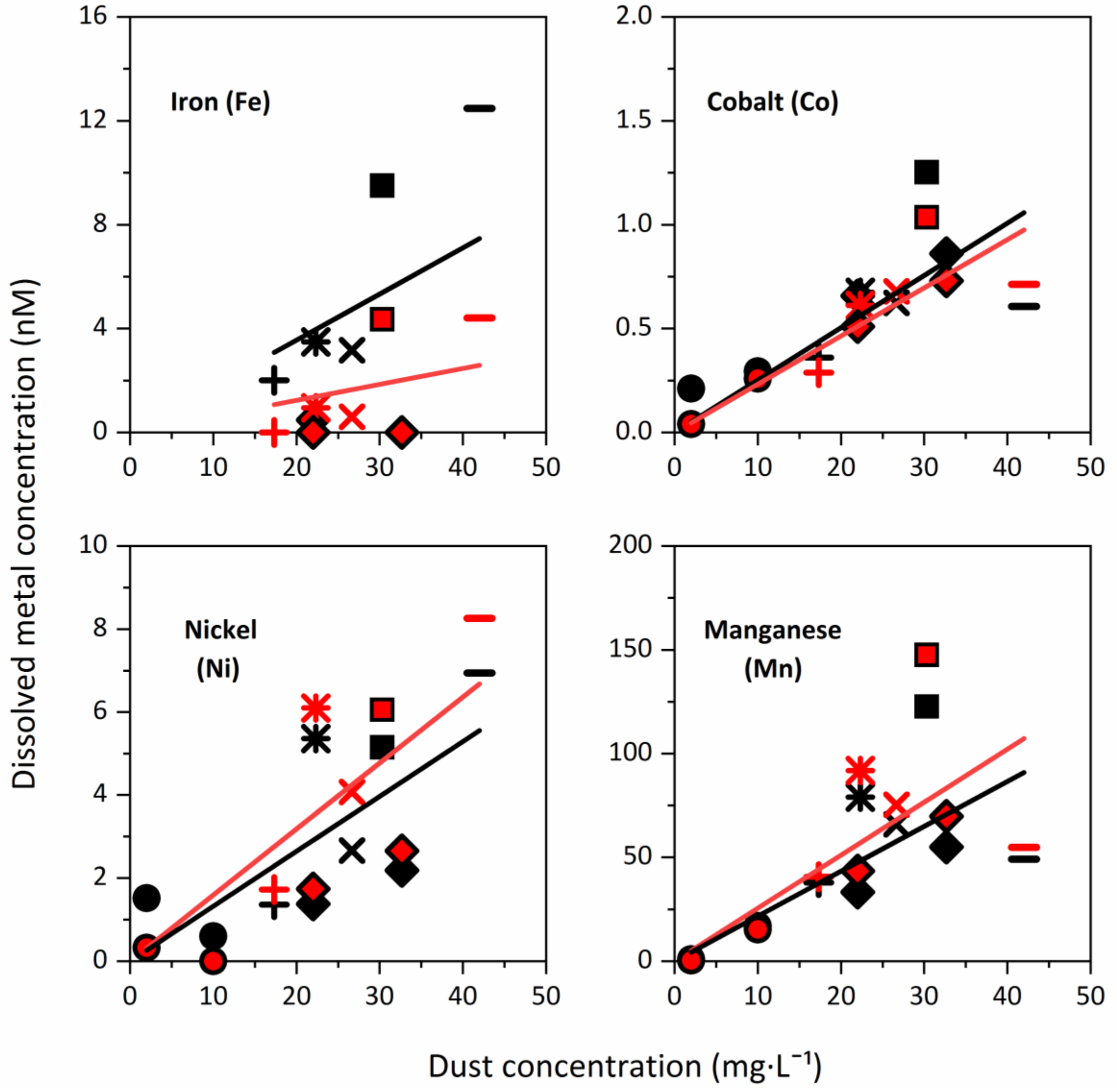

Metal (nM)	Regression slopes (nmol · (mg dust)$^{-1}$)			
	Fe	Co	Ni	Mn
Rapid diss.	0.18	0.025	0.13	2.16
Gradual diss.	0.06	0.023	0.16	2.55

Figure S6. The release kinetics of four additional metals (Fe, Co, Ni and Mn) in dust dissolution experiments, related to the main text - Fig. 4.

The dataset combines new measurements (circles) and published data from Mackey et al., 2015, which includes seven dust samples plotted as different symbols. Dissolution kinetics is presented in two categories - rapidly released metals (black, up to 6hrs) and gradually released metals (red, up to 7 days). A summary table of regression slopes is shown below.

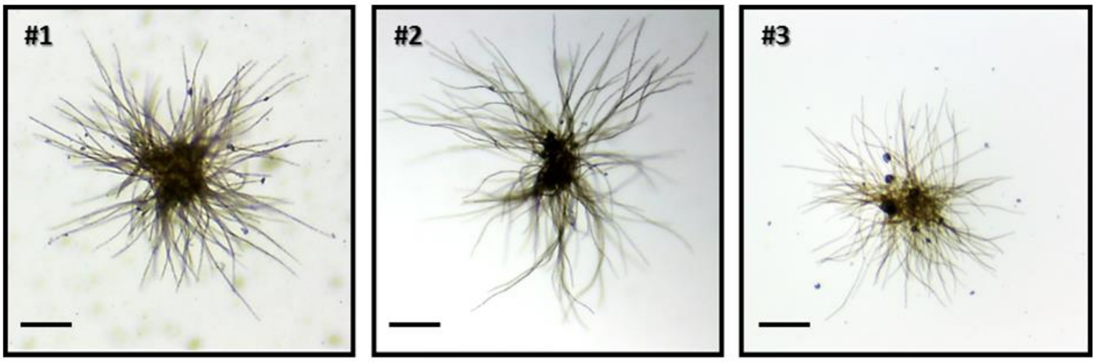

Colony	Colony radius	Colony volume	Dust load	Effective dust concn.
#	mm	mm^3; µL	ng	$mg \cdot L^{-1}$
1	0.410	0.29	69	239
2	0.689	1.37	675	492
3	0.381	0.23	214	925

Figure S7. Effective dust concentrations calculated for three representative natural/freshly collected Red Sea colonies, related to the main text section 3.2.2. The concentration ($mg \cdot L^{-1}$) was derived by dividing dust load (ng) by the colony volume (µL). Scale bar = 200 µm.

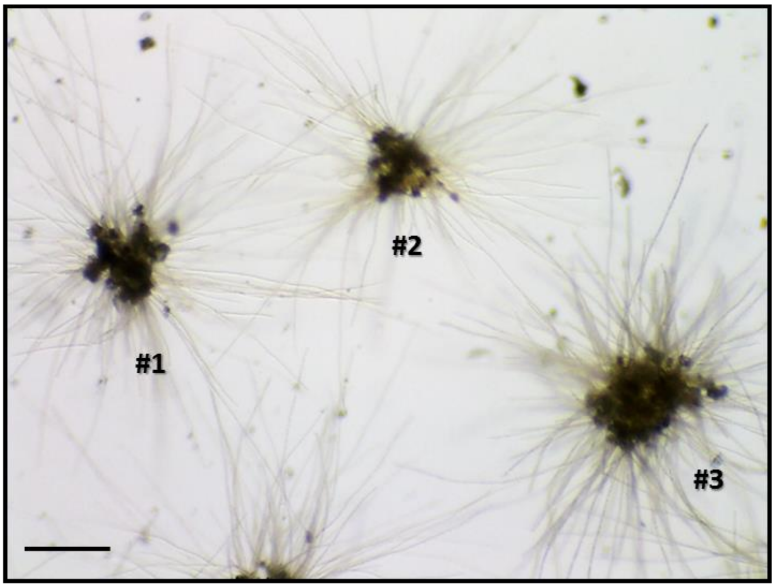

Colony	Incubation time	Colony radius	Colony volume	Dust load	Effective dust concn.
#	hours	mm	mm^3; µL	ng	$mg \cdot L^{-1}$
1	24	0.53	0.62	2490	4039
2	24	0.49	0.48	1948	4051
3	24	0.43	0.33	4127	12391

Figure S8. Images of Red Sea *Trichodesmium* colonies following a 24-hour *in situ* incubation with dust particles (10 $mg \cdot L^{-1}$). Effective dust concentrations within colony sphere were observed at levels exceeding 1000 $mg \cdot L^{-1}$. Scale bar = 200 µm.

Supplementary text S5. Characterizations of toxic particle removal via SEM-EDX analysis.

To investigate the ability of natural *Trichodesmium* colonies to remove toxic particles, incubation experiments were performed during the autumn of 2021, using 16 Red Sea colonies with Cu-containing mineral (malachite) and Fe-containing mineral (hematite). Briefly, 16 freshly collected colonies were first placed into a Nalgene bottle containing 2 mg·L^{-1} malachite and 2 mg·L^{-1} hematite (total particle concentration = 4 mg·L^{-1}). The bottle was then incubated *in situ* (under the pier of Interuniversity of Marine Science in Eilat, Israel) for up to 24 hrs. 5-6 colonies were subsampled at 2h, 6h and 24h, placed on a PES membrane filter (Supor®), air-dried and frozen prior to SEM-EDX analysis at Environmental Molecular Sciences Laboratory (EMSL), USA (Fig. S9a). Stereoscopic images of each colony after the incubation were taken prior to (Fig. S9b) and after the air-drying procedure (Fig. S9c), before SEM-EDX analysis.

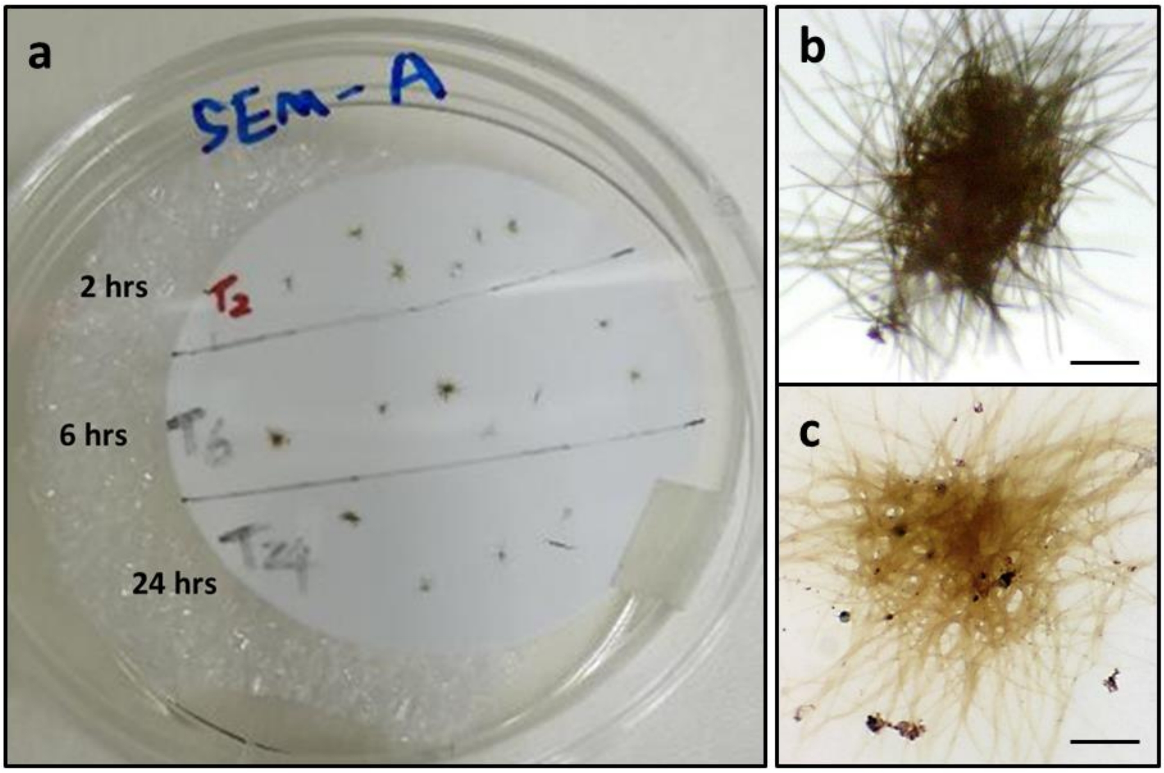

Figure S9. An illustrative figure of sample collection for SEM-EDX analysis (a), stereoscopic images of a colony prior to (b) and after the air-dried procedure (c). Scale bar = 200 µm.

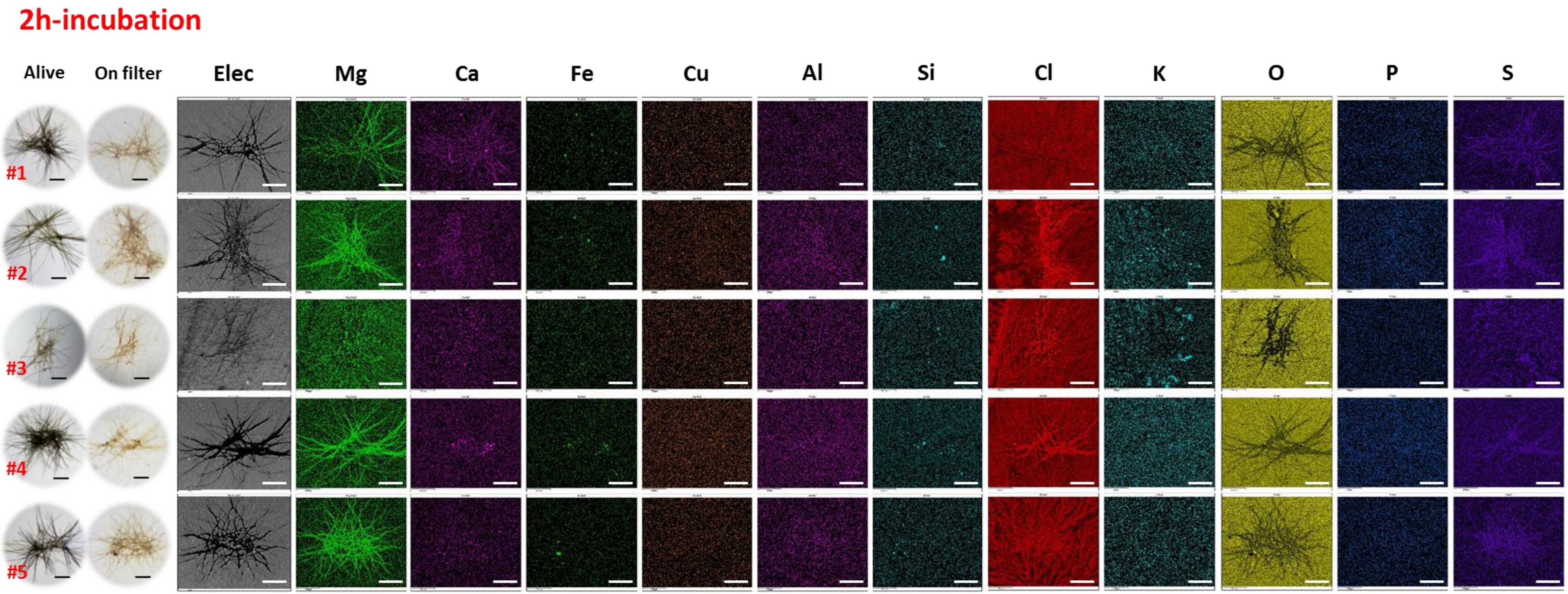

Figure S10. SEM-EDX images of five natural *Trichodesmium* colonies incubated with Cu-minerals (malachite) and Fe-minerals (hematite) for 2 hrs, related to the main text - Section 3.3.2. Stereoscopic images taken prior to (alive, 1st column) and after the air-drying procedure (on filter, 2nd column). "Elec" means electron. Scale bars for stereoscopic (1st and 2nd columns) and SEM images (3rd to 14th columns) are 200 and 250 µm, respectively.

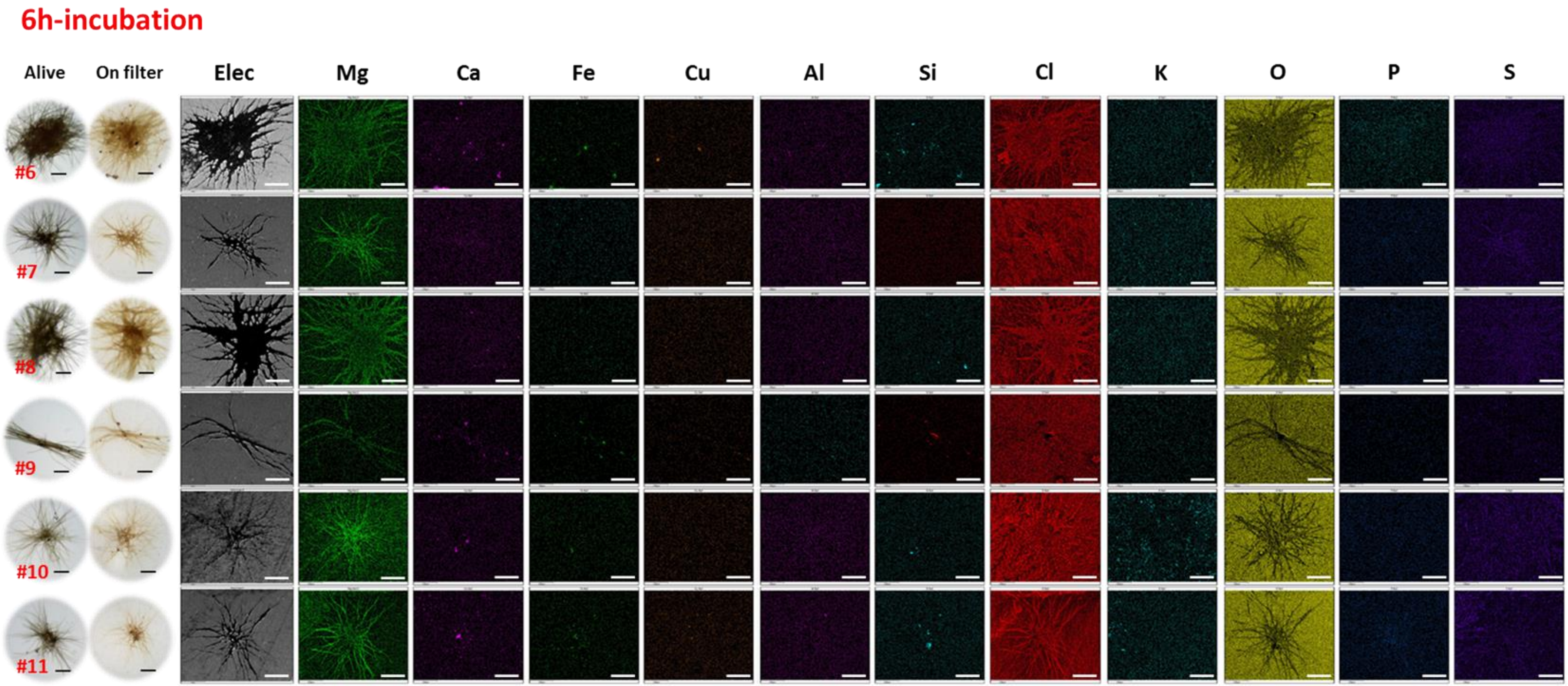

Figure S11. SEM-EDX images of five natural *Trichodesmium* colonies incubated with Cu-minerals (malachite) and Fe-minerals (hematite) for 6 hrs, related to the main text - Section 3.3.2. Stereoscopic images taken prior to (alive, 1st column) and after the air-drying procedure (on filter, 2nd column). "Elec" means electron. Scale bars for stereoscopic (1st and 2nd columns) and SEM images (3rd to 14th columns) are 200 and 250 µm, respectively. The element map (Mg, Ca, Fe and Cu) of colony (#11) was presented in the main text – Fig. 6 (top-left panel).

24h-incubation

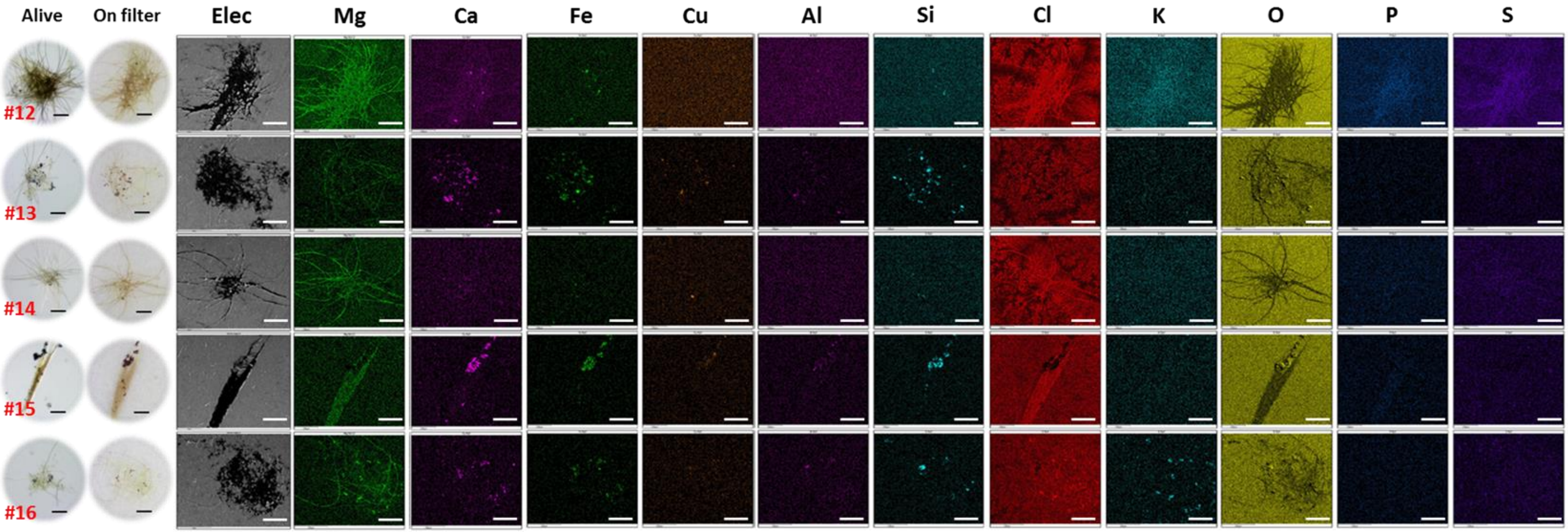

Figure S12. SEM-EDX images of five natural *Trichodesmium* colonies incubated with Cu-minerals (malachite) and Fe-minerals (hematite) for 24 hrs, related to the main text - Section 3.3.2. Stereoscopic images taken prior to (alive, 1st column) and after the air-drying procedure (on filter, 2nd column). "Elec" means electron. Scale bars for stereoscopic (1st and 2nd columns) and SEM images (3rd to 14th columns) are 200 and 250 µm, respectively. The element map (Mg, Ca, Fe and Cu) of colony (#13) was presented in the main text – Fig. 6 (top-right panel).

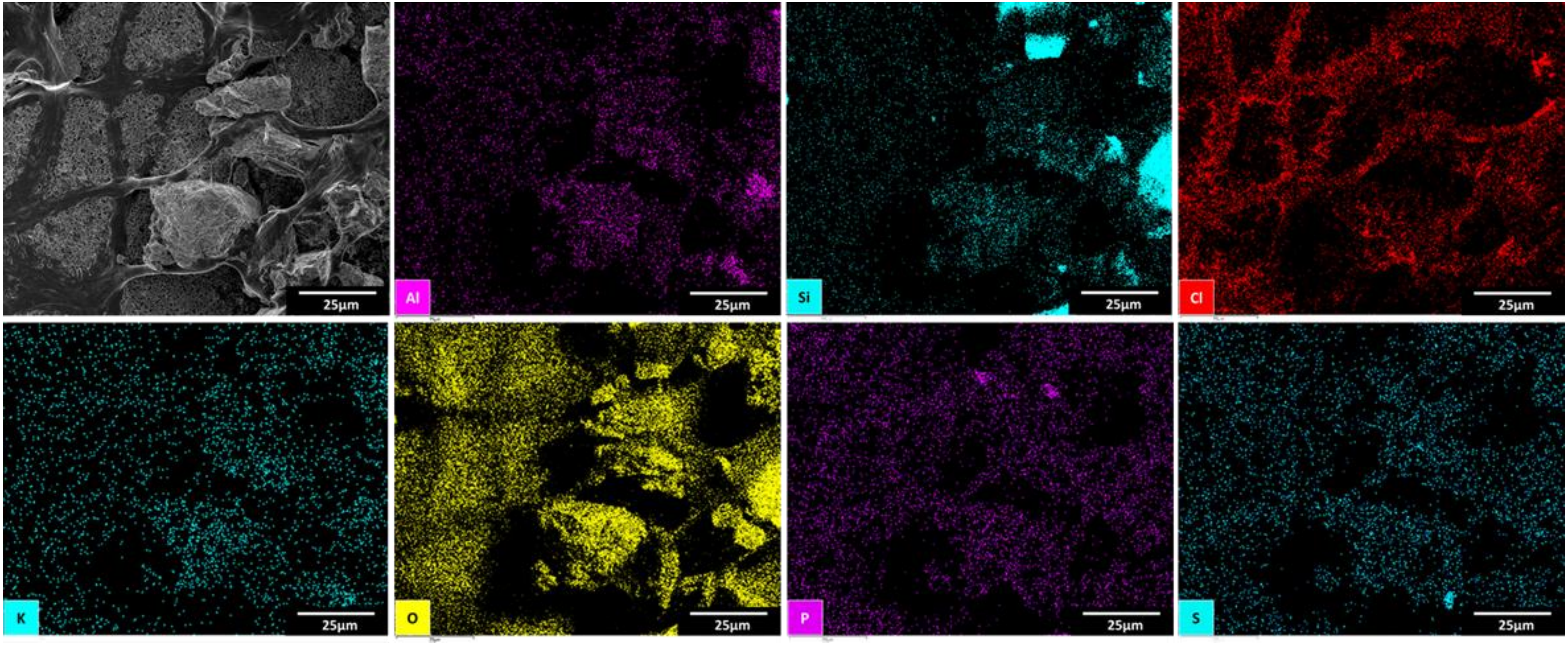

Figure S13. Additional element maps of a *Trichodesmium* colony (#13) incubated with Cu-minerals (malachite) and Fe-minerals (hematite) for 24 hrs, related to the main text - Section 3.3.2 (see Fig.6 – bottom panels). All scale bars = 25 µm.

References

Basu, S., & Shaked, Y. (2018). Mineral iron utilization by natural and cultured *Trichodesmium* and associated bacteria. *Limnology and Oceanography*, *63*(6), 2307–2320. https://doi.org/10.1002/lno.10939

Benaltabet, T., Lapid, G., & Torfstein, A. (2022). Dissolved aluminium dynamics in response to dust storms, wet deposition, and sediment resuspension in the Gulf of Aqaba, northern Red Sea. *Geochimica et Cosmochimica Acta*, *335*, 137–154. https://doi.org/10.1016/j.gca.2022.08.029

Benavides, M., Bonnet, S., Le Moigne, F. A. C., Armin, G., Inomura, K., Hallstrøm, S., et al. (2022). Sinking *Trichodesmium* fixes nitrogen in the dark ocean. *ISME Journal*, *16*(10), 2398–2405. https://doi.org/10.1038/s41396-022-01289-6

Held, N. A., Sutherland, K. M., Webb, E. A., McIlvin, M. R., Cohen, N. R., Devaux, A. J., et al. (2021). Mechanisms and heterogeneity of *in situ* mineral processing by the marine nitrogen fixer *Trichodesmium* revealed by single-colony metaproteomics. *ISME Communications*, *1*(1), 1–9. https://doi.org/10.1038/s43705-021-00034-y

Held, N. A., Waterbury, J. B., Webb, E. A., Kellogg, R. M., McIlvin, M. R., Jakuba, M., et al. (2022). Dynamic diel proteome and daytime nitrogenase activity supports buoyancy in the cyanobacterium *Trichodesmium*. *Nature Microbiology*, *7*(2), 300–311. https://doi.org/10.1038/s41564-021-01028-1

Ho, T. Y. (2013). Nickel limitation of nitrogen fixation in *Trichodesmium*. *Limnology and Oceanography*, *58*(1), 112–120. https://doi.org/10.4319/lo.2013.58.1.0112

Kromkamp, J., & Walsby, A. E. (1990). A computer model of buoyancy and vertical migration in cyanobacteria. *Journal of Plankton Research*, *12*(1), 161–183. https://doi.org/10.1093/plankt/12.1.161

Mackey, K. R. M., Chien, C. Te, Post, A. F., Saito, M. A., & Paytan, A. (2015). Rapid and gradual modes of aerosol trace metal dissolution in seawater. *Frontiers in Microbiology*, *6*(JAN), 1–11. https://doi.org/10.3389/fmicb.2014.00794

McConnell, C. L., Highwood, E. J., Coe, H., Formenti, P., Anderson, B., Osborne, S., et al. (2008). Seasonal variations of the physical and optical characteristics of saharan dust: Results from the dust outflow and deposition to the ocean (DODO) experiment. *Journal of Geophysical Research*, *113*, 1–19. https://doi.org/10.1029/2007JD009606

Paytan, A., Mackey, K. R. M., Chen, Y., Lima, I. D., Doney, S. C., Mahowald, N., et al. (2009). Toxicity of atmospheric aerosols on marine phytoplankton. *Proceedings of the National Academy of Sciences of the United States of America*, *106*(12), 4601–4605. https://doi.org/10.1073/pnas.0811486106

Schladitz, A., Müller, T., Kaaden, N., Massling, A., Kandler, K., Ebert, M., et al. (2009). *In situ* measurements of optical properties at Tinfou (Morocco) during the Saharan Mineral Dust Experiment SAMUM 2006. *Tellus, Series B: Chemical and Physical Meteorology*, *61*(1), 64–78. https://doi.org/10.1111/j.1600-0889.2008.00397.x

Sunda, W. G., & Huntsman, S. A. (1998). Processes regulating cellular metal accumulation and physiological effects: Phytoplankton as model systems. *Science of the Total Environment*, *219*(2–3), 165–181. https://doi.org/10.1016/S0048-9697(98)00226-5

Wang, S., Zhang, F., Koedooder, C., Qafoku, O., Basu, S., Krisch, S., et al. (2023). Calculations and simulations of dust factor (K) and sinking velocity of particle-free *Trichodesmium* colonies (v0). *Zenodo*. https://doi.org/10.5281/zenodo.10290901

White, A. E., Spitz, Y. H., & Letelier, R. M. (2006). Modeling carbohydrate ballasting by *Trichodesmium* spp. *Marine Ecology Progress Series*, *323*(Oliver 1994), 35–45. https://doi.org/10.3354/meps323035